

Non-adiabatic transitions in multi-level systems

Michael Wilkinson¹ and Michael A. Morgan²

¹ *Department of Physics and Applied Physics, John Anderson Building, University of Strathclyde, Glasgow, G4 0NG, UK.*

² *Department of Physics, Seattle University, Seattle, WA 98122, U.S.A.*
(November 26, 2021)

Abstract

In a quantum system with a smoothly and slowly varying Hamiltonian, which approaches a constant operator at times $t \rightarrow \pm\infty$, the transition probabilities between adiabatic states are exponentially small. They are characterized by an exponent that depends on a phase integral along a path around a set of branch points connecting the energy level surfaces in complex time. Only certain sequences of branch points contribute. We propose that these sequences are determined by a topological rule involving the Stokes lines attached to the branch points. Our hypothesis is supported by theoretical arguments and results of numerical experiments.

University of Washington preprint NT@UW-98-26

PACS numbers: 03.65Ge, 03.65Sq.

arXiv:quant-ph/9908018v1 4 Aug 1999

Typeset using REVTeX

Contents

I	Introduction	2
II	A topological rule for determining the actions	5
	A Adiabatic solutions of the Schrödinger equation	5
	B Solutions in the neighborhood of a branch point	6
	C Transition probabilities deduced from Heading's rule	8
	D The case of two branch points	9
	E A criterion for selecting possible transition sequences	11
III	Adiabatic renormalization with projections	11
	A Motivation for renormalizing the Hamiltonian	11
	B Renormalization excluding a subspace	12
	C Iteration of the transformation	14
IV	Interpretation of the asymptotic series	16
	A Form of the Hamiltonian at large order, excluding projected subspace . .	16
	B Form of the Hamiltonian at large order, including projected subspace . .	17
	C Interpretation of the renormalized Hamiltonian	18
V	Numerical illustration	19
VI	Concluding remarks	21
VII	Acknowledgements	22

I. INTRODUCTION

Consider a quantum mechanical system with a Hamiltonian $\hat{H}(X)$ that depends analytically on a parameter X and has a discrete spectrum. Suppose the parameter changes slowly and analytically with time t , in such a way that asymptotically as $t \rightarrow \pm\infty$, it remains constant. It is convenient to write $X = X(\tau)$ where $\tau = \epsilon t$. The *adiabatic parameter* ϵ is a small, real number which provides a dimensionless measure of how slowly the Hamiltonian changes, due to the change in the parameter X . The quantum adiabatic theorem states that if such a system is prepared in the n^{th} eigenstate of the instantaneous Hamiltonian at any time, then in the limit $\epsilon \rightarrow 0$, the system remains in the n^{th} eigenstate of the instantaneous Hamiltonian at later times [1,2].

Corrections to the adiabatic theorem can be extremely small. If $X(\tau)$ approaches its limiting values sufficiently rapidly as $\tau \rightarrow \pm\infty$, the probability of making a transition to another eigenstate of the Hamiltonian vanishes exponentially (faster than any power of ϵ) as $\epsilon \rightarrow 0$. The probability for making a transition from the state $|\phi_n(X(\tau_0))\rangle$ to the state $|\phi_m(X(\tau_f))\rangle$ is given asymptotically in ϵ by

$$P_{n \rightarrow m} \sim C_{nm} \exp[-2S_{nm}/\hbar] \tag{1.1}$$

where C_{nm} and S_{nm} are positive constants and the action S_{nm} is inversely proportional to ϵ . Results of this type have been proven rigorously for most cases of physical interest in which the Hamiltonian is a 2×2 [3,4] or 3×3 matrix [5,6], and for some special cases of multi-level systems [7-10]. This paper will discuss how these constants S_{nm} , C_{nm} describing non-adiabatic transitions may be determined with some generality for a discrete multi-level system. For definiteness, we will assume that the Hamiltonian \hat{H} is a symmetric $\mathcal{N} \times \mathcal{N}$ matrix, which is real for real τ , and analytic on a strip containing the real τ axis. Then the Schwartz reflection principle guarantees conjugacy of the matrix elements about the real time axis.

The special case of a two-level system has been discussed by many authors. Zener [3] calculated an exact expression for the transition probability for a two level model of the form

$$\hat{H}(X) = \frac{1}{2} \begin{pmatrix} X & \Delta \\ \Delta & -X \end{pmatrix}, \quad X = A\tau . \quad (1.2)$$

This Landau-Zener system is of particular importance because for a multi-level system, according to degenerate perturbation theory, a near-degeneracy or ‘avoided crossing’ of two levels can be approximated by a two-state Hamiltonian of this form. The exact transition probability for this system is

$$P_{LZ} = \exp(-\pi\Delta^2/2A\epsilon\hbar) . \quad (1.3)$$

Note that the closest approach of the energy levels $E(t)$ is Δ , so that non-adiabatic transitions occur easily if the energy levels approach each other closely.

Later Dykhne [4] showed that in the limit $\epsilon \rightarrow 0$ the transition probability for a general two level system is determined entirely by the analytic continuation of the energy levels as a function of complex time. The eigenvalues of the instantaneous Hamiltonian $E(\tau)$ form two branches of a single complex function, which are connected at branch points occurring as complex conjugate pairs. The action exponent S is determined by integrating the energy along a path which leaves the real axis and loops around a branch point so that it returns on the other branch. Dykhne showed that, in the limit $\epsilon \rightarrow 0$, the transition probability becomes

$$P \sim \exp\left[-\frac{2}{\hbar} \left| \text{Im} \int_{\gamma} dt E(t) \right| \right] \equiv \exp[-2S/\hbar] \quad (1.4)$$

where γ is the path illustrated in figure 1. The prefactor in (1.1) is seen to be $C = 1$. If there are more than one pair of branch points, the one with the smallest value of S gives the dominant contribution to the transition probability. For the model (1.2), $S = \pi\Delta^2/4\epsilon A$, so that the Landau-Zener formula follows from this more general result.

In a multi-level system, it is natural to expect that the transition probability is, in general, the product of several terms of the form of (1.4), corresponding to several successive transitions between pairs of levels. The conclusions of this paper will confirm this expectation. It might also be expected that the transition probability will be determined by the combination of paths around branch points that minimizes the total value of the sum of integrals S of the form appearing in (1.4). This expectation is only partially correct: not all sequences of branch points are allowed. In this paper we propose a topological constraint, or rule, that the allowed combinations of branch points should satisfy. The value of S is determined by

the minimal value of the sum of integrals of the form (1.4) for paths consistent with the constraint.

An heuristic reason for the necessity of a rule that eliminates certain sequences of branch points can be understood from an example given by Hwang and Pechukas [5]. Consider a three level system, with energy levels as plotted schematically in figure 2(a). There are two avoided crossings where pairs of levels approach each other very closely. In the neighborhood of these avoided crossings the two nearly degenerate levels can be represented by a two-state model similar to (1.2), and the transition probabilities between pairs of adjacent levels are determined by the branch points near the real axis shown in figure 2(b). The transitions from level 1 to level 3 occur through Landau-Zener transitions at the successive avoided crossings, and the transition probability is the product of two terms of the form of (1.4). The transition from level 3 to level 1 cannot make use of the same path, however, because the avoided crossing between levels 2 and 1 is encountered before the transition from level 3 to level 2 has taken place. Instead, the transition occurs through a more distant branch point between levels 1 and 3 as shown in figure 2(b). The probability for the $3 \rightarrow 1$ transition is therefore expected to be much smaller. Therefore, a rule is required that eliminates the path from level 3 to level 1 via the branch points closest to the real axis, but permits this path for the reversed transition.

In section 2 a rule is proposed for determining which branch points contribute to the transition probabilities. Our rule is motivated by a discussion of the Stokes phenomenon given by Heading [11,12], which assumes that evanescent waves are meaningful even in the presence of larger contributions, and that the amplitudes of evanescent waves change on the Stokes lines. These assumptions must be justified by a reference to an asymptotic series in ϵ for the wavefunction, showing that the errors in the dominant terms can be reduced to below the magnitude of the subdominant (evanescent) terms, except in the vicinity of the Stokes lines. This interpretation of the asymptotic series for the wavefunction occurs in Stokes' analysis of the Airy function [13], and many further examples are discussed in a book by Dingle [14]. Works by Berry [15-17] have developed the theory further and discuss physical applications, including quantum adiabatic theory for two-level systems.

The standard approaches for this interpretation of Stokes lines are valid only for those Stokes lines associated with branch points having the smallest action S , since these give the most divergent contributions to the asymptotic series. All applications to date have considered systems with only two states (in adiabatic theory) or two channels (in WKB approaches to scattering problems), where only this one branch point is relevant. These methods are bound to fail in multi-level systems where many branch points are of necessity involved in a transition, since the divergence of the series is dominated by the branch point with the smallest action. In section 3 we describe a formulation that allows all of the Stokes lines to be given a similar interpretation. By projecting out the subspace corresponding to branch points with small actions, divergences due to other branches are revealed. The method is based upon an exact iterative 'renormalization' of the Hamiltonian, adapted from a scheme introduced by Berry [18]. Section 4 discusses the limiting form of this series of renormalized Hamiltonian operators and its interpretation in terms of the Stokes phenomenon. Section 5 contains some numerical illustrations of the results, and section 6 summarizes the new contributions and considers further development of the theory.

II. A TOPOLOGICAL RULE FOR DETERMINING THE ACTIONS

In this section we propose a topological rule for determining the actions for non-adiabatic transitions motivated by a discussion of the Stokes phenomenon. The first three subsections review some ideas well known in the context of WKB theory. We review these ideas here to place them in the slightly different context of adiabatic theory and to establish our notation.

A. Adiabatic solutions of the Schrödinger equation

It is possible to write down an asymptotic series for the solution of the Schrödinger equation $i\hbar \partial_t |\psi(t)\rangle = \hat{H}(t)|\psi(t)\rangle$ as an expansion in powers of ϵ

$$|\psi_n(t)\rangle = \exp[-i\theta_n(t, t_0)/\hbar] \left\{ |\phi_n(\tau)\rangle + \epsilon |\phi_n^{(1)}(\tau)\rangle + \dots + \epsilon^k |\phi_n^{(k)}(\tau)\rangle + \dots \right\} \quad (2.1)$$

where $|\phi_n(\tau)\rangle$ is an eigenvector of the instantaneous Hamiltonian $\hat{H}(X(\tau))$, and $\theta_n(t, t_0)$ is the phase integral of the corresponding eigenvalue (n^{th} energy level) defined by

$$\theta_n(t, t_0) = \int_{t_0}^t dt' E_n(t') = \frac{1}{\epsilon} \int_{\tau_0}^{\tau} d\tau E_n(\tau) , \quad (2.2)$$

with t_0 the phase reference. The state in (2.1) is an approximate solution of the time-dependent Schrödinger equation, assuming the system was prepared in the n^{th} energy level in the remote past, that doesn't take into account non-adiabatic transitions. Only the leading order terms in these asymptotic expansions will be considered explicitly. These will be termed the *adiabatic solutions*

$$|\psi_n(t)\rangle = \exp[-i\theta_n(t, t_0)/\hbar] |\phi_n(t)\rangle . \quad (2.3)$$

For complex t , the exponential factor need not have unit modulus. As we move along a path in the complex t plane, we can compare the rate at which two solutions increase or decrease exponentially. The solution for which the derivative of $\text{Im} \theta_n$ is largest is said to be *dominant* and the other solution *subdominant*.

Because the solutions are to be considered as functions of a complex time variable, it is necessary to include a few comments about how the eigenvalues and eigenvectors are continued into the complex plane. Since for real t the matrix elements of the Hamiltonian are real, we define the inner product of two eigenvectors without complex conjugation. We shall assume that the eigenvectors are normalized in the usual way, using this inner product. As t becomes complex, the eigenvalues and eigenvectors also become complex, but the Hamiltonian matrix remains symmetric and its eigenvectors orthogonal. By choosing the eigenvectors real on the real axis, they then have no gauge freedom. They may be expressed as analytic functions of t at all points in the complex plane, except for a set of singular points.

Singular points of the eigenvalues and eigenvectors can arise either because the matrix elements themselves have singularities, or because of singularities in the mapping from matrix elements to eigenvalues and eigenvectors. This latter type of singularity is associated with points where eigenvalues become degenerate in the complex t plane. These singularities arising from degeneracies will be termed *branch points*, because they connect two branches

of the Riemann surface of the eigenvalue function $E(t)$. The former type of singularities are of less interest, because they are not universal in form, and because they typically lie farther into the complex plane than the branch points. (The reason for this will be discussed in section 5.) Degenerate perturbation theory shows that in the neighborhood of two eigenvalues becoming degenerate, the energy difference is the square root of the discriminant of the corresponding quadratic equation. At the singularity, the discriminant vanishes while, generically, its time rate of change is non-zero. Thus generically, singularities due to eigenvalue degeneracies are square-root branch points. In this paper we shall assume all relevant singularities are of this form.

For systems with a single parameter X , assumed here, a theorem of Von Neumann and Wigner [19] states that, generically, degeneracies do not occur for real t . Therefore the eigenvalues and eigenvectors can be labeled with an index corresponding to the ordering of the (real) eigenvalues on the real axis. Usually it will be useful to consider the eigenvalues and eigenvectors to be single-valued functions of t . This requires the introduction of branch cuts that restrict the domain of definition of the function $E(t)$ to a single Riemann sheet. Typically we will choose the branch cuts to be lines with constant $\text{Re } t$ that do not cross the real axis, as illustrated in figure 2(b).

It is necessary to establish how the eigenvalues and eigenvectors change upon crossing a branch cut. Consider a branch point due to the degeneracy $E_{n_1} = E_{n_2}$. Since this is a square-root branch point, the eigenvalues are simply exchanged as the branch cut is traversed. The eigenvectors are more involved. If, starting from a point t_+ adjacent to the branch cut, the eigenvector $|\phi_{n_1}(t_+)\rangle$ is followed anticlockwise around the branch point, upon reaching the other side of the branch point the state $|\phi_{n_1}(t_-\rangle$ is equal to a multiple of the state $|\phi_{n_2}(t_+)\rangle$. This is illustrated in figure 3(a). Upon taking this multiple of the state $|\phi_{n_2}(t_+)\rangle$ anticlockwise to t_- , it is transformed into $-|\phi_{n_1}(t_+)\rangle$, i.e., the eigenvector recurs with its sign changed after two circuits around the degeneracy. This fact is easily verified in the special case of the Landau-Zener model, (1.2). Choose a branch cut crossing the real axis connecting the complex conjugate branch points, and consider a circuit constructed from the real axis and from a semicircle at infinity, as illustrated in figure 3(b). Because the circuit can be shrunk to a circle enclosing the branch point, and because the singularities of this model are generic, the result is true in the general case. Thus if we choose the phase of the state $|\phi_{n_2}\rangle$ relative to $|\phi_{n_1}\rangle$ appropriately, we may write

$$\begin{aligned} |\phi_{n_1}(t_-\rangle &= i|\phi_{n_2}(t_+)\rangle \\ |\phi_{n_2}(t_-\rangle &= i|\phi_{n_1}(t_+)\rangle \end{aligned} \tag{2.4}$$

as a generic description of how the eigenvectors change when crossing a branch cut in the anticlockwise sense.

B. Solutions in the neighborhood of a branch point

This section considers the solution of the Schrödinger equation in the vicinity of a branch point. The arguments are an adaptation of those given by Heading [11,12] for the case of WKB approximations. They are included here because the terminology must be re-defined for the adiabatic problem, and because there is a minor difference in the logic.

We assume that at t^* the levels E_{n_1} and E_{n_2} become degenerate. In the neighborhood of t^* the difference between the two nearly degenerate levels behaves as $\Delta E \equiv E_{n_2} - E_{n_1} \approx \text{const.}(t - t^*)^{1/2}$, so that the phase integral difference has a singularity of the form

$$\Delta\theta(t, t^*) = \int_{t^*}^t dt' \Delta E(t') \approx \frac{K_{t^*}}{\epsilon} (\tau - \tau^*)^{3/2} \quad (2.5)$$

where K_{t^*} is a complex constant characterizing the branch point at t^* . Thus it is also necessary to introduce branch cuts in the phase integrals $\theta_n(t, t^*)$, which we take to be the same as for the energies. On crossing a branch cut we must change the labeling of the energy levels and phase integrals, although their values change smoothly.

Some of the level curves (contours) of the phase integral that pass through the branch point are very important in the formulation of the theory. These are the Stokes and anti-Stokes lines defined by

$$\begin{aligned} \text{Re } \Delta\theta = 0 & \quad \text{Stokes lines} \\ \text{Im } \Delta\theta = 0 & \quad \text{anti - Stokes lines .} \end{aligned} \quad (2.6)$$

On the anti-Stokes lines the solutions (2.3) connected by the branch point are co-dominant, and on the Stokes lines one solution can be regarded as being maximally dominant over the other. The Stokes lines associated with a typical branch point are sketched in figure 4.

The subdominant solution is meaningful only if it is larger than the error term of the dominant series, which can itself be assumed to be comparable to the smallest term of the asymptotic expansion (2.1). On considering how the solution behaves near a branch point, it is convenient to first consider the behavior of the solution on the anti-Stokes lines. This is because the adiabatic series corresponding to the two levels which become degenerate at the branch point are co-dominant on the anti-Stokes lines, and are therefore certainly both meaningful there. If these solutions are $|\psi_1(t)\rangle$, $|\psi_2(t)\rangle$, the solution at any point along the anti-Stokes line (A1) in figure 4 may be written

$$|\psi(t)\rangle = \alpha_1 |\psi_1(t)\rangle + \alpha_2 |\psi_2(t)\rangle \quad (2.7)$$

with the multipliers α_1 , α_2 approximately constant. On the other two anti-Stokes lines the solution takes the same form, but it need not have the same coefficients; for example, on line (A2) the coefficients could be (α'_1, α'_2) . Since the Schrödinger equation is linear, there must be a linear relationship between the coefficients on the anti-Stokes lines:

$$\begin{pmatrix} \alpha'_1 \\ \alpha'_2 \end{pmatrix} = \tilde{M} \begin{pmatrix} \alpha_1 \\ \alpha_2 \end{pmatrix} . \quad (2.8)$$

If $|\psi_1(t)\rangle$ is the dominant solution in the sector between the lines (A1) and (A2), then the multiplier of this solution cannot change, i.e., $\alpha'_1 = \alpha_1$. Heading [11,12] has given a very general argument, showing that the multiplier of the subdominant solution is altered on crossing the Stokes line. For the generic case, where the singularity is given by (2.5) (triplets of Stokes lines attached to a branch point), the argument follows closely that given by Heading for the WKB approximation and the result is the same: the transition matrix from the anti-Stokes line (A1) to (A2) is

$$\tilde{M} = \begin{pmatrix} 1 & 0 \\ -i & 1 \end{pmatrix} . \quad (2.9)$$

In other words, $-i$ times the multiplier of the dominant solution is added to that of the subdominant solution whenever a Stokes line is crossed in the anticlockwise sense. This is *Heading's rule*. It assumes a phase reference at the branch point. Similar relations exist on crossing the other Stokes lines. However, in writing down expressions for these relations it should be remembered that, on crossing anti-Stokes lines, it is possible for the dominance of the solutions to switch. For example, if $|\psi_2(t)\rangle$ is dominant on both (S2) and (S3), then dominance switches upon crossing (A1) and (A2) but not (A3). The exact solution of the time-dependent Schrödinger equation must be analytic and single valued at the branch point, so equation (2.9) is obtained by requiring that the multipliers α_i return to their original values when traced in a circuit around the branch point, crossing three Stokes lines and the branch cut. The branch cut is accounted for by noting that, according to (2.4), upon crossing the cut the labels of the states are exchanged and the states are multiplied by i (this circumstance differs from the case of WKB theory, where the factors of i have a different origin). We can introduce the matrix

$$\tilde{T} = \begin{pmatrix} 0 & 1 \\ 1 & 0 \end{pmatrix} \quad (2.10)$$

to account for the switching of dominance on the anti-Stokes lines. The branch cut is accounted for by the matrix $i\tilde{T}$. The effect of making a circuit around the branch point is then described by the product $i\tilde{T}\tilde{M}\tilde{T}\tilde{M}\tilde{T}\tilde{M}$, which is the identity matrix, verifying that (2.9) is consistent with a single-valued wavefunction.

It is desirable to comment on the interpretation of (2.9). The adiabatic wavefunctions are a poor approximation to the exact solution at the branch point because they are singular there. They are also a poor approximation far away from the branch point because of the presence of other branch points and singularities. Furthermore, their interpretation is ambiguous at all points off the anti-Stokes lines, because the subdominant wavefunction may be smaller than the error of the dominant wavefunction. As they stand then, the arguments above suffice only to discuss the behavior of the wavefunction in a (deleted) neighborhood of the branch point, near the anti-Stokes lines.

C. Transition probabilities deduced from Heading's rule

The results of section 2.2 are sufficient to enable the transition probability due to a single branch point to be determined, provided that they are supplemented by an additional assumption. The logic of the argument presented in section 2.2 gives the form of the wavefunction on two of the anti-Stokes lines, provided it is known on the third (and even on the anti-Stokes lines it is only a good approximation sufficiently far from the branch point). The additional assumption is that the solutions may be extended from the anti-Stokes lines as required and still remain meaningful. This assumption requires the use of asymptotic series approximations, which reduce the errors of the dominant terms until the subdominant terms are meaningful. Such approximations are not discussed explicitly in Heading's work and must be verified for specific applications.

It will be convenient to introduce the following notation for the phase integral factor in the

adiabatic solutions:

$$f_n(t, t_0) \equiv \exp[-i\theta_n(t, t_0)/\hbar] = \exp\left[-\frac{i}{\hbar} \int_{t_0}^t dt' E_n(t')\right]. \quad (2.11)$$

We assume that the system begins in the state $|\psi_1(t)\rangle = f_1(t, t_0)|\phi_1(t)\rangle$ as $t \rightarrow -\infty$. The phase reference t_0 is an arbitrary point on the real axis. As $t \rightarrow \infty$, the system evolves to the state $|\psi_1(t)\rangle + a|\psi_2(t)\rangle$, where a is the transition amplitude that we seek. In the domain in figure 4 bounded between (A1), (S1) and the real axis, the system is in the dominant state with respect to the branch point in the upper-half plane. Heading's rule, given by (2.8) and (2.9), gives the evolution of the solution around the branch point from (A1) to (A2) as

$$f_1(t, t^*)|\phi_1(t)\rangle \rightarrow f_1(t, t^*)|\phi_1(t)\rangle - if_2(t, t^*)|\phi_2(t)\rangle, \quad (2.12)$$

or in terms of the adiabatic solutions with phase reference t_0 as

$$f_n(t_0, t^*)|\psi_1(t)\rangle \rightarrow f_1(t_0, t^*)|\psi_1(t)\rangle - if_2(t_0, t^*)|\psi_2(t)\rangle. \quad (2.13)$$

Assuming we may extend this solution down to time t on the real axis, the probability for the system to be found in state $|\psi_2(t)\rangle$ is

$$P_{1 \rightarrow 2} \sim |f_2(t_0, t^*)f_1(t^*, t_0)|^2 = \exp[-2 \text{Im} S_{1,2}/\hbar] \quad (2.14)$$

where

$$S_{1,2} \equiv \int_{t_0}^{t^*} dt' [E_2(t') - E_1(t')] = - \int_{\gamma} dt' E(t') \quad (2.15)$$

is the action evaluated around a path, analogous to that shown in figure 1, encircling the branch point at t^* . Its value is independent of the phase reference t_0 . Thus Dykhne's formula (1.4) has been deduced from Heading's rule.

Note that the branch point below the real axis does not make any contribution to this transition probability, because the solution $|\psi_1\rangle$ is subdominant in the lower half plane. To compute the transition probability for transitions in the opposite direction, the roles of the two conjugate branch points are reversed.

D. The case of two branch points

In this section we discuss the case in which a transition occurs in two stages, first from the level n_0 to level n_1 , and then from level n_1 to level n_2 . Consideration of this case allows us to identify a rule for determining the circumstances under which successive transitions may occur.

We examine a case in which adjacent pairs of levels become degenerate at distinct branch points. If we are concerned with transitions from lower to higher energies, branch points in the upper half plane are relevant, because for paths below these branch points lower lying levels are dominant. The Stokes lines (defined by (2.6)) of the two branch points can assume two possible arrangements as illustrated schematically in figures 5(a),(b).

First consider the arrangement in figure 5(a), with the initial state being such that only the level with index n_0 is occupied as $t \rightarrow -\infty$. Following the argument used in the last section,

we use Heading's rule to connect the solutions on the anti-Stokes lines in the vicinity of the branch points, and assume that these solutions may be extended down to the real time axis. Since only the initial state $|\psi_{n_0}(t)\rangle$ occupies the sector between the lines (A1) and (S1) attached to the branch point (n_0, n_1) , and since $|\psi_{n_0}(t)\rangle$ is the dominant solution on (S1), Heading's rule gives the wavefunction on (A2) as a multiple of $|\psi_{n_0}(t)\rangle - i|\psi_{n_1}(t)\rangle$. Thus the evolution of the solution around the (n_0, n_1) branch point from (A1) to (A2) is given by

$$f_{n_0}(t, t_{n_0, n_1}^*)|\phi_{n_0}(t)\rangle \rightarrow f_{n_0}(t, t_{n_0, n_1}^*)|\phi_{n_0}(t)\rangle - if_{n_1}(t, t_{n_0, n_1}^*)|\phi_{n_1}(t)\rangle. \quad (2.16)$$

Next, since no Stokes lines are intervening, we may extend this solution upward to the anti-Stokes line (A1') connected to the (n_1, n_2) branch point. The sector between (A1') and (S1') is now occupied by the solution $|\psi_{n_1}(t)\rangle$. Since this is the dominant solution on (S1'), Heading's rule gives the wavefunction on (A2') as a multiple of $|\psi_{n_1}(t)\rangle - i|\psi_{n_2}(t)\rangle$. The evolution of the solution around the (n_1, n_2) branch point from (A1') to (A2') is given by

$$f_{n_1}(t, t_{n_1, n_2}^*)|\phi_{n_1}(t)\rangle \rightarrow f_{n_1}(t, t_{n_1, n_2}^*)|\phi_{n_1}(t)\rangle - if_{n_2}(t, t_{n_1, n_2}^*)|\phi_{n_2}(t)\rangle. \quad (2.17)$$

Combining these two evolutions, and expressing the result in terms of the adiabatic solutions with a phase reference t_0 on the real axis, one obtains

$$\begin{aligned} |\psi_{n_0}(t)\rangle &\rightarrow |\psi_{n_0}(t)\rangle - if_{n_1}(t_0, t_{n_0, n_1}^*)f_{n_0}(t_{n_0, n_1}^*, t_0)|\psi_{n_1}(t)\rangle \\ &\quad - f_{n_2}(t_0, t_{n_1, n_2}^*)f_{n_1}(t_{n_1, n_2}^*, t_{n_0, n_1}^*)f_{n_0}(t_{n_0, n_1}^*, t_0)|\psi_{n_2}(t)\rangle \end{aligned} \quad (2.18)$$

for the evolution of the wavefunction from (A1) to (A2'). Extending this solution down to time t on the real axis, one finds the probability for making the transition from level n_0 to level n_2 is

$$\begin{aligned} P_{n_0 \rightarrow n_2} &\sim |f_{n_2}(t_0, t_{n_1, n_2}^*)f_{n_1}(t_{n_1, n_2}^*, t_{n_0, n_1}^*)f_{n_0}(t_{n_0, n_1}^*, t_0)|^2 \\ &= |f_{n_2}(t_0, t_{n_1, n_2}^*)f_{n_1}(t_{n_1, n_2}^*, t_0)f_{n_1}(t_0, t_{n_0, n_1}^*)f_{n_0}(t_{n_0, n_1}^*, t_0)|^2 \\ &= \exp[-2 \operatorname{Im}(S_{n_0, n_1} + S_{n_1, n_2})/\hbar] \end{aligned} \quad (2.19)$$

where S_{n_0, n_1} and S_{n_1, n_2} are actions for paths evaluated around the branch points located at times t_{n_0, n_1}^* and t_{n_1, n_2}^* , respectively. The transition probability is therefore the product of two factors of the Dykhne formula form, corresponding to two successive transitions.

Now consider the arrangement in figure 5(b) with the same initial state $|\psi_{n_0}(t)\rangle$ occupied as $t \rightarrow -\infty$. At the (n_1, n_2) branch point, $|\psi_{n_1}(t)\rangle$ is dominant and $|\psi_{n_2}(t)\rangle$ is subdominant. According to Heading's rule, a transition into the n_2 level requires that the subdominant solution be switched on in proportion to the dominant solution's multiplier. However, the solution $|\psi_{n_1}(t)\rangle$ has multiplier zero in the entire region containing the relevant anti-Stokes lines attached to the (n_1, n_2) branch point. It follows that no transition from n_0 to n_2 is possible using these two branch points.

There usually will be other branch points farther out in the complex plane connecting levels n_0 and n_2 directly. In both of the cases discussed above, this branch point would make a contribution to the transition probability of the form $P_{n_0 \rightarrow n_2} = P_{n_2 \rightarrow n_0} = \exp[-2 \operatorname{Im} S_{n_0, n_2}/\hbar]$. In the case of figure 5(b), this would be the only contribution. In the case of figure 5(a), it is the dominant contribution if $\operatorname{Im} S_{n_0, n_2} < \operatorname{Im} S_{n_0, n_1} + \operatorname{Im} S_{n_1, n_2}$, and negligible otherwise.

E. A criterion for selecting possible transition sequences

We now propose a rule for determining the combinations of actions that correspond to allowed transitions. The rule is based upon Heading's local analysis of the form of the solution in the vicinity of a branch point, supplemented by the assumption that solutions may be continued away from the branch points.

In the case of an upward transition from level n_0 to n_k , a transition might be possible using a sequence of branch points $t_{n_0, n_1}^*, t_{n_1, n_2}^*, \dots, t_{n_{k-1}, n_k}^*$ with transition probability $P_{n_0 \rightarrow n_k} = \exp[-2 \text{Im}(S_{n_0, n_1} + \dots + S_{n_{k-1}, n_k})/\hbar]$. This *transition sequence* is allowed only if the branch points and their associated Stokes lines satisfy a topological criterion. The transition $n_j \rightarrow n_{j+1}$ is mediated by the branch point at $t_{n_j, n_{j+1}}^*$, and can occur only if the level n_j is occupied at this branch point. This requires that the branch point $t_{n_j, n_{j+1}}^*$ lies in the quarter plane above the real axis, and to the right of the boundary formed by the Stokes line descending from t_{n_{j-1}, n_j}^* to cross the real axis, and the branch cut from the t_{n_{j-1}, n_j}^* branch point.

The rule is topological in character. For downward transitions, the relevant branch points are in the lower-half plane, but because of reflection symmetry, the rule can be applied in exactly the same way as for upward transitions. The rule might at first sight appear to have a degree of arbitrariness, in that it refers to the positions of the branch cuts as well as the Stokes lines. It may, however, be verified that moving the branch cuts does not affect the predictions. The reason is that when a branch cut from the t_{n_0, n_1}^* branch point is moved past the t_{n_1, n_2}^* branch point, the labeling of the levels must be changed so that the latter branch point now connects levels n_0 and n_2 rather than n_1 and n_2 .

III. ADIABATIC RENORMALIZATION WITH PROJECTIONS

A. Motivation for renormalizing the Hamiltonian

The objective of this section is to explain how the interpretation of the Stokes lines used in section 2, which led to the rule for the selection of transition sequences, may be justified. This requires the use of asymptotic series to reduce the error of the dominant solutions as far as possible. It turns out that this error can be reduced below the magnitude of the subdominant solution everywhere, except in the vicinity of the Stokes lines. This idea was introduced by Stokes [13] in a discussion of the Airy function and amplified in a book by Dingle [14]. It has been applied successfully in a variety of forms and to a variety of physical problems by Berry [15-17]. To date, all of the applications to differential equations have involved problems in which only two equations are coupled together, e.g., two-state problems in adiabatic theory, or one-dimensional semiclassical problems, involving two channels (left and right propagating waves).

The approach used in these papers must be generalized to cover the multi-level problem. The reason is that the interpretation of the Stokes lines depends on studying the divergence of an asymptotic series. This divergence is usually determined by the branch point 'closest' to the real axis, in the sense of having the smallest value of the imaginary part of the action, $|\text{Im} S|$. A means must be found to eliminate the divergence associated with branch points close to the real axis in order that the divergence associated with other branch points may be revealed, allowing their Stokes lines to be interpreted. This is achieved by 'projecting

out' a subspace of the Hilbert space spanned by states having branch points close to the real axis.

Various approaches were tried and found to be unsatisfactory. The method we use is adapted from an approach introduced by Berry [18]. Instead of constructing an asymptotic series for the wavefunction, the objective is to construct a sequence of 'renormalized' Hamiltonians having the same dynamics as the original problem and for which the adiabatic approximation is successively more accurate. The k^{th} Hamiltonian of this sequence has off-diagonal matrix elements of $O(\epsilon^k)$. If the off-diagonal elements were to approach zero as $k \rightarrow \infty$, the adiabatic approximation would be exact. In this case there would be no non-adiabatic transitions. This implies that the prefactors of the $O(\epsilon^k)$ terms must diverge as $k \rightarrow \infty$. This divergence and its consequences are discussed in section 4. In the remainder of this section we explain how the sequence of renormalized Hamiltonians is constructed. The approach follows that of Berry [18] quite closely, except that a subspace of the spectrum is 'projected out' of the renormalization procedure, leaving its elements $O(\epsilon^0)$.

B. Renormalization excluding a subspace

We consider a case where there is a branch point close to the real axis in a subset of the spectrum characterized by a set of state indices $\{P\}$. The projection operator $\hat{P}(t)$ for the corresponding sub-space of the Hilbert space is

$$\hat{P}(t) = \sum_{n \in P} |\phi_n(t)\rangle \langle \phi_n(t)| . \quad (3.1)$$

The complementary set of state indices will be termed $\{Q\}$ and its corresponding projection operator designated $\hat{Q} = \hat{I} - \hat{P}$. Provided the singularities of the matrix elements of the Hamiltonian are sufficiently far from the real axis, the singularities of the projection operator \hat{P} are determined by the branch points where an eigenvalue from $\{P\}$ becomes degenerate with one from $\{Q\}$. The projection operator $\hat{P}(t)$ and the projected Hamiltonian $\hat{H}_P = \hat{P}\hat{H}\hat{P}$ are analytic inside a strip Σ_P symmetric about the real axis and bounded by these conjugate branch points. This is true despite the fact that the eigenstates in (3.1) have singularities closer to the real axis due to branch points between states in $\{P\}$.

It will be useful to have available a representation of the projection into the $\{P\}$ subspace explicitly constructed from analytic quantities. To this end a set of states $|\chi_n(t)\rangle$, $n \in \{P\}$ will be constructed having no singularities inside the strip Σ_P and satisfying

$$\langle \chi_n(t) | \chi_{n'}(t) \rangle = \delta_{nn'} , \quad \hat{P}(t) | \chi_n(t) \rangle = | \chi_n(t) \rangle , \quad \lim_{t \rightarrow \pm\infty} | \chi_n(t) \rangle = | \phi_n(\pm\infty) \rangle . \quad (3.2)$$

This set of states could be constructed explicitly in one of several ways. As an example, consider the smooth interpolation

$$\frac{1}{2}(|\phi_n(+\infty)\rangle + |\phi_n(-\infty)\rangle) + \frac{1}{2}(|\phi_n(+\infty)\rangle - |\phi_n(-\infty)\rangle) \tanh(\epsilon t) . \quad (3.3)$$

These state vectors could then be projected into the subspace by multiplication by \hat{P} and then orthogonalized by a Gram-Schmidt procedure.

Consider the unitary operator

$$\hat{U}_0(t) = \sum_{n \in P} |\chi_n(t)\rangle \langle \chi_n(-\infty)| + \sum_{n \in Q} |\phi_n(t)\rangle \langle \phi_n(-\infty)| \quad (3.4)$$

which generates the states at t from the states at $t = -\infty$. In order to simplify notation, the states $|\tilde{\phi}_n(t)\rangle$ will be used to denote the states $|\chi_n(t)\rangle$ for $n \in \{P\}$ and $|\phi_n(t)\rangle$ for $n \in \{Q\}$ so that (3.4) is

$$\hat{U}_0(t) = \sum_n |\tilde{\phi}_n(t)\rangle \langle \tilde{\phi}_n(-\infty)| . \quad (3.5)$$

Following Berry [18], we introduce a new representation $|\psi_1(t)\rangle$ of the solution of the time-dependent Schrödinger equation defined by

$$|\psi(t)\rangle = \hat{U}_0(t)|\psi_1(t)\rangle . \quad (3.6)$$

This renormalized wavefunction satisfies the Schrödinger equation

$$i\hbar \partial_t |\psi_1\rangle = \hat{H}_1 |\psi_1\rangle \quad (3.7)$$

with the renormalized Hamiltonian given by

$$\hat{H}_1(t) = \hat{U}_0^\dagger(t) \hat{H}(t) \hat{U}_0(t) - i\hbar \hat{U}_0^\dagger(t) \partial_t \hat{U}_0(t) . \quad (3.8)$$

The matrix elements of \hat{H}_1 are conveniently evaluated in the basis formed by the eigenvectors at $t \rightarrow -\infty$

$$H_{nm}^{(1)} \equiv \langle \phi_n(-\infty) | \hat{H}_1 | \phi_m(-\infty) \rangle = \langle \tilde{\phi}_n(t) | \hat{H} | \tilde{\phi}_m(t) \rangle - i\hbar \langle \tilde{\phi}_n(t) | \partial_t \tilde{\phi}_m(t) \rangle . \quad (3.9)$$

Three different cases arise. In the case where n and m are both in $\{Q\}$

$$H_{nm}^{(1)} = \delta_{nm} E_n(t) - i\hbar \frac{\langle \phi_n(t) | \partial_t \hat{H}(t) | \phi_m(t) \rangle}{E_m(t) - E_n(t)} (1 - \delta_{nm}) , \quad (n, m \in \{Q\}) \quad (3.10)$$

and for n, m both in $\{P\}$

$$H_{nm}^{(1)} = \langle \chi_n(t) | \hat{H}(t) | \chi_m(t) \rangle - i\hbar \langle \chi_n(t) | \partial_t \chi_m(t) \rangle , \quad (n, m \in \{P\}) . \quad (3.11)$$

The case $n \in \{P\}, m \in \{Q\}$ requires some discussion. The state $|\partial_t \phi_m(t)\rangle$ may be written

$$|\partial_t \phi_m(t)\rangle = \sum_{n \in \{P\}} a_n |\chi_n(t)\rangle + \sum_{n \in \{Q\}} a_n |\phi_n(t)\rangle . \quad (3.12)$$

Differentiating the Schrödinger equation $(\hat{H} - E_m)|\phi_m\rangle = 0$ with respect to time, then multiplying by $\langle \chi_l |$ gives the following linear equations for the a_n with $n \in \{P\}$

$$\sum_{n \in \{P\}} D_{ln} a_n = b_l , \quad (3.13)$$

where

$$D_{ln} \equiv E_m \delta_{ln} - \langle \chi_l | \hat{P} \hat{H} \hat{P} | \chi_n \rangle , \quad b_l \equiv \langle \chi_l | \partial_t \hat{H} | \phi_m \rangle . \quad (3.14)$$

It is useful to define a matrix \tilde{G} that is the inverse of $\tilde{D} = \{D_{ln}\}$, and a corresponding operator \hat{G}

$$\hat{G}(t) \equiv \sum_{l,n \in \{P\}} |\chi_l(t)\rangle G_{ln}(t) \langle \chi_n(t)| = (E_m - \hat{P}\hat{H}\hat{P})^{-1}. \quad (3.15)$$

Using the fact that $\tilde{G} = \{G_{ln}\}$ is the inverse of \tilde{D} , one finds the solution of (3.13) is

$$\begin{aligned} a_l &= \langle \chi_l | \partial_t \phi_m \rangle = \sum_{n \in \{P\}} G_{ln} \langle \chi_n | \partial_t \hat{H} | \phi_m \rangle \\ &= \sum_{n \in \{P\}} \langle \chi_l | (E_m - \hat{P}\hat{H}\hat{P})^{-1} | \chi_n \rangle \langle \chi_n | \partial_t \hat{H} | \phi_m \rangle. \end{aligned} \quad (3.16)$$

It follows that

$$H_{nm}^{(1)} = -i\hbar \langle \chi_n(t) | (E_m - \hat{P}\hat{H}\hat{P})^{-1} \hat{P} \partial_t \hat{H} | \phi_m(t) \rangle, \quad (n \in \{P\}, m \in \{Q\}). \quad (3.17)$$

In summary, the matrix elements of the renormalized Hamiltonian are given by the expressions in (3.10), (3.11), and (3.17). Notice that all of the off-diagonal elements are $O(\epsilon)$, except those in the $n, m \in \{P\}$ block, which are $O(1)$, and that $H_{nm}^{(1)}(t)$ is diagonal as $t \rightarrow \pm\infty$, because the original Hamiltonian is constant in both limits.

C. Iteration of the transformation

The renormalization transformation defined in the last section can be iterated by writing successive wavefunctions and Hamiltonian operators as

$$|\psi_k(t)\rangle = \hat{U}_k(t) |\psi_{k+1}(t)\rangle, \quad \hat{H}_{k+1} = \hat{U}_k^\dagger \hat{H}_k \hat{U}_k - i\hbar \hat{U}_k^\dagger \partial_t \hat{U}_k. \quad (3.18)$$

Note that the transformation of the Hamiltonian is valid for any choice of the unitary operator \hat{U}_k . The operators $\hat{U}_k(t)$ will be defined by

$$\hat{U}_k(t) = \sum_n |\tilde{\phi}_n^{(k)}(t)\rangle \langle \tilde{\phi}_n^{(k)}(-\infty)| \quad (3.19)$$

where

$$\begin{aligned} (\hat{H}_k - E_n^{(k)}) |\phi_n^{(k)}\rangle &= 0, \quad (n \in \{Q\}) \\ \hat{P}_k |\chi_n^{(k)}\rangle &= |\chi_n^{(k)}\rangle, \quad \langle \chi_n^{(k)}(t) | \chi_{n'}^{(k)}(t) \rangle = \delta_{nn'}, \quad (n, n' \in \{P\}). \end{aligned} \quad (3.20)$$

Here the new projection operator \hat{P}_k is defined in analogy to (3.1) using the new instantaneous eigenstates $|\phi_n^{(k)}\rangle$ for $n \in \{P\}$. The notation $|\tilde{\phi}_n^{(k)}(t)\rangle$ is used to denote the states $|\chi_n^{(k)}(t)\rangle$ for $n \in \{P\}$ and $|\phi_n^{(k)}(t)\rangle$ for $n \in \{Q\}$. Since both $H_{nm}^{(1)}(\pm\infty)$ are diagonal, we have $|\tilde{\phi}_n^{(1)}(\pm\infty)\rangle = |\phi_n(-\infty)\rangle$. The $|\chi_n^{(k)}(t)\rangle$ are chosen so that they are analytic in the strip Σ_{P_k} and close to the $|\phi_n(-\infty)\rangle$ as $t \rightarrow \pm\infty$. As in the last section for the $k = 0$ case, these states can be generated by acting on linear combinations of the $|\phi_n(\pm\infty)\rangle$ with the projection operator $\hat{P}_k(t)$, then using a Gram-Schmidt procedure to create orthonormalized

states. It is still most convenient to evaluate matrix elements of the Hamiltonian \hat{H}_k with respect to the states $|\phi_n(-\infty)\rangle$. Generalizing the equations in section 3.2, the matrix elements $H_{nm}^{(k+1)} \equiv \langle \phi_n(-\infty) | \hat{H}_{k+1}(t) | \phi_m(-\infty) \rangle$ are given by

$$H_{nm}^{(k+1)} = \delta_{nm} E_n^{(k)}(t) - i\hbar \frac{\langle \phi_n^{(k)}(t) | \partial_t \hat{H}_k(t) | \phi_m^{(k)}(t) \rangle}{E_m^{(k)}(t) - E_n^{(k)}(t)} (1 - \delta_{nm}), \quad (n, m \in \{Q\}) \quad (3.21a)$$

$$= \langle \chi_n^{(k)}(t) | \hat{H}_k(t) | \chi_m^{(k)}(t) \rangle - i\hbar \langle \chi_n^{(k)}(t) | \partial_t \chi_m^{(k)}(t) \rangle, \quad (n, m \in \{P\}) \quad (3.21b)$$

$$= -i\hbar \langle \chi_n^{(k)}(t) | (E_m^{(k)} - \hat{P}_k \hat{H}_k \hat{P}_k)^{-1} \hat{P}_k \partial_t \hat{H}_k | \phi_m^{(k)}(t) \rangle. \quad (n \in \{P\}, m \in \{Q\}) \quad (3.21c)$$

After k stages of iteration all matrix elements are $O(\epsilon^k)$, except the diagonal elements and all of the elements of the PP block, which remain $O(1)$. Each Hamiltonian is an exact representation of the dynamics of the original problem, and the transition amplitudes could, in principle, be obtained by integrating the Schrödinger equation with any Hamiltonian in the sequence. At each stage the $H_{nm}^{(k)}(\pm\infty)$ are diagonal and hence $|\tilde{\phi}_n^{(k)}(\pm\infty)\rangle = |\phi_n(-\infty)\rangle$. The amplitude for transition from state n to state m is therefore given by $\langle \phi_m(\infty) | \psi_n(\infty) \rangle = \langle \phi_m(-\infty) | \psi_{k,n}(\infty) \rangle$, where $|\psi_n(t)\rangle$ and $|\psi_{k,n}(t)\rangle$ are the wavefunctions obtained by propagating the initial state $|\phi_n(-\infty)\rangle$ with Hamiltonians \hat{H} and \hat{H}_k , respectively. If the $O(\epsilon^k)$ matrix elements vanished as $k \rightarrow \infty$ there would be no non-adiabatic transitions. Therefore, the sequence of renormalized Hamiltonians is expected to have the typical behavior for terms of an asymptotic series, in that, although the matrix elements decrease for small k , at sufficiently large k they diverge because of a faster than exponential growth of the prefactors. The value of k for which the largest of the small matrix elements has smallest magnitude will be denoted by $k^*(\epsilon)$. This divergence will be examined in greater detail in section 4.

For small ϵ and for large values of k which are not too large, the off-diagonal matrix elements outside the PP block are very small. Thus, for states in $\{Q\}$, the approximations

$$|\phi_n^{(k)}(t)\rangle \sim |\phi_n(-\infty)\rangle, \quad E_n^{(k)}(t) \sim E_n(t), \quad (\epsilon \ll 1, \quad 1 \ll k \leq k^*, \quad n \in \{Q\}) \quad (3.22a)$$

are valid, while for states in $\{P\}$ we are at liberty to choose

$$|\chi_n^{(k)}(t)\rangle \sim |\phi_n(-\infty)\rangle, \quad (\epsilon \ll 1, \quad 1 \ll k \leq k^*, \quad n \in \{P\}). \quad (3.22b)$$

From this, along with (3.11) and (3.21b), it follows that for small ϵ

$$\langle \chi_n^{(k)}(t) | \hat{H}_k(t) | \chi_m^{(k)}(t) \rangle \sim \langle \chi_n(t) | \hat{H}(t) | \chi_m(t) \rangle, \quad (n, m \in \{P\}). \quad (3.23)$$

When these approximations are valid, equations (3.21) simplify considerably. The basis states are approximately time independent, so the derivatives with respect to the Hamiltonian become derivatives with respect to matrix elements

$$H_{nm}^{(k+1)} \sim \delta_{nm} E_n(t) - i\hbar \frac{\partial_t [H_{nm}^{(k)}(t)]}{E_m(t) - E_n(t)} (1 - \delta_{nm}), \quad (n, m \in \{Q\}) \quad (3.24a)$$

$$\sim H_{nm}^{(k)}(t), \quad (n, m \in \{P\}) \quad (3.24b)$$

$$\sim -i\hbar \sum_{l \in \{P\}} G_{nl} \partial_t [H_{lm}^{(k)}], \quad (n \in \{P\}, m \in \{Q\}). \quad (3.24c)$$

To summarize: equations (3.21) describe an exact renormalization of the Hamiltonian, which for sufficiently large (but not too large) k , has the effect of reducing the magnitude of all of the off-diagonal elements outside the PP block. Equations (3.24) are an approximate implementation of this iteration valid for sufficiently small ϵ .

IV. INTERPRETATION OF THE ASYMPTOTIC SERIES

All of the renormalized Hamiltonians \hat{H}_k describe the same dynamics. In particular $|\langle \phi_m(-\infty) | \psi_{k,n}(\infty) \rangle|^2$, where $|\psi_{k,n}(t)\rangle$ is the wavefunction propagated under the Hamiltonian \hat{H}_k from the initial state $|\phi_n(-\infty)\rangle$, is the transition probability from state n to state m and is independent of k . Now the viewpoint of section 2, which associates transitions between pairs of levels with Stokes lines, will be confirmed here by showing that when k is suitably large, the Hamiltonian $\hat{H}_k(t)$ on the real axis is greatest at crossings of Stokes lines [17]. Section 4.1 examines the case where there is no projected subspace: a direct generalization of the result for two level systems. Section 4.2 considers the extension to the case where there is a projected subspace, showing that the Stokes lines can still have the same significance for branch points not close to the real axis. Section 4.3 describes how these results can be used to calculate a transition probability involving a sequence of branch points.

A. Form of the Hamiltonian at large order, excluding projected subspace

This section discusses the form of the matrix elements of the renormalized Hamiltonian in the limit where $\epsilon \ll 1$ and $1 \ll k \leq k^*$. Equation (3.24a) which determines the evolution of off-diagonal matrix elements in the QQ block, is an iteration of the form

$$H_{k+1}(t) = -\frac{i\hbar}{\Delta(t)} \partial_t H_k(t) \quad (4.1)$$

where $H_1(t)$ and $\Delta(t)$ are given functions. From observations on asymptotic series discussed by Dingle [14] it is well known that for large k , solutions of (4.1) may be obtained in the form

$$H_k(t) \sim (-1)^k A \Gamma(k + \gamma) [F(t)]^{-(k+\gamma)} \quad (4.2)$$

where A and γ are constants, and $\Gamma(x)$ is the Gamma function satisfying $\Gamma(x+1) = x\Gamma(x) \equiv x!$. Substitution of (4.2) into (4.1) shows that the dimensionless scalar function $F(t)$ is

$$F(t) = \frac{i}{\hbar} \int_{t^*}^t dt' \Delta(t'), \quad (4.3)$$

and the lower limit t^* will sometimes be shown explicitly as $F(t, t^*)$. The possible values of t^* are determined by realizing that an acceptable solution of (4.1) should be regular at any point for which $\Delta^{-1}(t)$ and $H_1(t)$ are regular. The solution (4.2) is clearly divergent for $k + \gamma > 0$ when $t \rightarrow t^*$. This observation implies that t^* must correspond to a singular point, where at least one of $\Delta^{-1}(t)$ and $H_1(t)$ has non-analytic behavior. In the context of adiabatic theory t^* corresponds to a branch point singularity.

In general, the solution at time t is dominated by the approximate solution (4.2) attached to a singular point t^* for which the modulus of $F(t, t^*)$ is smallest. Since equation (4.1) is linear, a superposition of co-dominant solutions of the form (4.2) may be necessary. In the case where the functions $H_1(t)$ and $\Delta^{-1}(t)$ are analytic and real valued on the real axis, the singular points occur as complex conjugate pairs. In this situation the solution on the real axis is a superposition of solutions with conjugate singularities.

In our application where $\Delta = (E_m - E_n)$, the real part of F is constant along the real axis. Thus, on the real axis, the magnitude of the solution (4.2) is largest at the point where the Stokes line, defined by $\text{Im } F(t, t^*) = 0$, crosses. For large k the magnitude decays rapidly, with an approximately gaussian form on either side of this point. When the two conjugate solutions are combined, the result is a real function with oscillations within an approximately gaussian envelope.

The constants A and γ can be determined - although they are not required for application of the theory. Both constants are obtained by considering the behavior of the functions in the neighborhood of the singularity. In the application of these results to adiabatic theory, equation (3.10) requires that the function $H_1(t)$ plays the role of $\langle \phi_n(t) | \partial_t \hat{H} | \phi_m(t) \rangle / (E_m(t) - E_n(t))$, which scales as $c(t - t^*)^{-1}$ in the vicinity of a branch point singularity at t^* . In the vicinity of the branch point, the form of the successive $H_k(t)$ is dominated by the components of $H_1(t)$ and $\Delta^{-1}(t)$ which are most strongly divergent as $t \rightarrow t^*$. It is therefore appropriate to take $H_1(t) = c(t - t^*)^{-1}$ and $\Delta(t) = \alpha(t - t^*)^{1/2}$. This leads by direct application of (4.1) to a general form for the $H_k(t)$ valid in the neighborhood of t^*

$$H_k(t) = C_k (t - t^*)^{-(3k-1)/2}, \quad C_{k+1} = -\frac{3k-1}{2\alpha} C_k. \quad (4.4)$$

The iteration for the coefficients C_k has a solution

$$C_k = \left(\frac{-3}{2\alpha} \right)^{k-1} \frac{\Gamma(k - \frac{1}{3})}{\Gamma(\frac{2}{3})} c. \quad (4.5)$$

Comparison of this result with (4.2) shows that they are consistent in the limit $k \rightarrow \infty$, and that $\gamma = -\frac{1}{3}$ and $A = -(\frac{2\alpha}{3})^{\frac{2}{3}} c / \Gamma(\frac{2}{3})$.

Applying these results to the renormalization of the QQ block of the Hamiltonian (equation (3.24a)), shows that for large k the off-diagonal matrix elements are largest for the element $H_{nm}^{(k)}$ for which $|F|$ is smallest. On the real axis $F = iS_{nm}/\hbar$, so this corresponds to the matrix element with the least $|\text{Im } S_{nm}|$. Furthermore, each of these matrix elements is largest in the vicinity of the point where the Stokes line intersects the real axis. The most significant process in the dynamics of \hat{H}_k is therefore a transition between levels n and m localized in time at the point where the Stokes line crosses the real axis. The use of the renormalization scheme therefore confirms the interpretation that the transition occurs at the Stokes line. The results are consistent with the conclusions of section 2, and we will assume that the transition probability is given by (2.14) and (2.15).

B. Form of the Hamiltonian at large order, including projected subspace

In the case where there is a sub-space projected out in the manner discussed in section 3, the equation for the iteration of the off-diagonal matrix elements in the QQ block is exactly

of the form considered in section 4.1 above. The case of matrix elements in the PQ and QP blocks requires a different treatment. The equation for iteration of these elements of the Hamiltonian is of the form (3.24c), which we write symbolically as

$$\tilde{H}_{k+1}(t) = -i\hbar \tilde{G}(t) \partial_t \tilde{H}_k(t) \quad (4.6)$$

where \tilde{H}_k is a column vector of dimension \mathcal{N}_P , with elements $H_{nm}^{(k)}$, and $\tilde{G} = \{G_{nl}\} = \{\langle \chi_n | (E_m - \hat{P}\hat{H}\hat{P})^{-1} | \chi_l \rangle\}$, a matrix of dimension $\mathcal{N}_P \times \mathcal{N}_P$. Note that the index m is fixed and not shown in (4.6). Following (4.2), it might be anticipated that a solution of (4.6) is of the form

$$\tilde{H}_k = (-1)^k \Gamma(k + \gamma) [\tilde{M}(t)]^{-(k+\gamma)} \tilde{A}, \quad (4.7)$$

where $\tilde{M}(t)$ is a matrix of dimension $\mathcal{N}_P \times \mathcal{N}_P$ and \tilde{A} a constant column vector of dimension \mathcal{N}_P . We proceed to show that (4.7) is the solution to (4.6) to leading order in k^{-1} . Let $\tilde{M}(t) = \tilde{X}^{-1}(t) \tilde{F}(t) \tilde{X}(t)$, where $\tilde{F}(t)$ is diagonal. Then the time derivative may be simplified using the following approximation valid to leading order in k^{-1} :

$$\partial_t [\tilde{M}(t)]^{-k} = -k \tilde{X}^{-1}(t) \partial_t \tilde{F}(t) [\tilde{F}(t)]^{-(k+1)} \tilde{X}(t) + O(1). \quad (4.8)$$

Using this approximation one finds that (4.7) is the solution to (4.6) to leading order in k^{-1} so long as $-i\hbar \tilde{X} \tilde{G} \tilde{X}^{-1} \partial_t \tilde{F}$ is the identity matrix. It follows that $\tilde{X} \tilde{G} \tilde{X}^{-1}$ must be diagonal since \tilde{F} is assumed to be diagonal. The matrix $\tilde{X}(t)$ is therefore the similarity transformation that diagonalizes $\tilde{G}(t)$, and the matrix $\tilde{F}(t)$ and its elements $F_n(t)$ are

$$\begin{aligned} \tilde{F}(t) &= \frac{i}{\hbar} \int_{t^*}^t dt' \tilde{X}(t') \tilde{G}(t')^{-1} \tilde{X}^{-1}(t') \\ F_n(t) &= \frac{i}{\hbar} \int_{t^*}^t dt' [E_m(t') - E_n(t')]. \end{aligned} \quad (4.9)$$

Substitution into (4.7) now gives the required approximation. These results are a natural generalization of the results for the simpler case described by the iteration (4.1). A similar argument to that given in section 4.1 forces t^* to be the position of a singularity, where a pair of eigenvalues, one each from the P and Q subspaces, become degenerate.

It is worth noting that these expressions can be simplified by making use of freedom available in the specification of the states $|\chi_n(t)\rangle$. The states $|\chi_n(t)\rangle$ may be chosen to coincide with the eigenstates $|\phi_n(t)\rangle$ at isolated positions in the complex time plane, so that the similarity transformation $\tilde{X}(t)$ is the identity at that point. Specifically, these states may be chosen to coincide at the point where a Stokes line crosses the real axis. The comments in section 4.1, indicating how the renormalized Hamiltonian is concentrated on Stokes lines, can then be applied equally well to this case: from (4.7) and (4.9) it can be seen that the dominant term in the high-order renormalized Hamiltonian comes from the branch point with the smallest value of $|\text{Im} S_{nm}|$, where at least one of n, m is in the Q subspace. If $\tilde{X}(t)$ is the identity where the corresponding Stokes line crosses the real axis, the largest matrix elements determine the transition between states n and m .

C. Interpretation of the renormalized Hamiltonian

As an example of how these considerations can be used to demonstrate the validity of the topological rule, consider their application to the case of two successive transitions $n_0 \rightarrow n_1$

followed by $n_1 \rightarrow n_2$. It will be assumed that the (n_0, n_1) branch point is closest to the real axis and that the (n_1, n_2) branch point is next closest. The subspace P is then chosen to be that spanned by levels n_0, n_1 . The states $|\chi_{n_0}(t)\rangle$ and $|\chi_{n_1}(t)\rangle$ are chosen to correspond to the eigenstates $|\phi_{n_0}(t)\rangle$ and $|\phi_{n_1}(t)\rangle$ at the point t_S where the Stokes line from the (n_1, n_2) branch point crosses the real axis. When the order k is sufficiently large, the matrix elements that determine transitions from the P subspace are largest for the transition between levels n_1 and n_2 , and are concentrated at t_S . The general arguments given in section 2 indicate that this transition probability is $P_{n_1 \rightarrow n_2} \sim \exp[-2 \text{Im } S_{n_1, n_2}/\hbar]$.

The probability for making a transition from state n_0 to n_2 via the intermediate state n_1 therefore depends on the dynamics within the PP sub-block at times earlier than t_S . The matrix elements within this sub-block have been left approximately unchanged by iteration of the renormalization procedure. Any suitable procedure can be used to calculate the probability for the transition $n_0 \rightarrow n_1$ occurring before the time t_S . In the limit $\epsilon \rightarrow 0$, the most convenient procedure is of course to use adiabatic theory that predicts the transition will occur on the Stokes line attached to the (n_0, n_1) branch point with the probability $P_{n_0 \rightarrow n_1} \sim \exp[-2 \text{Im } S_{n_0, n_1}/\hbar]$. The overall transition probability for the $n_0 \rightarrow n_2$ transition going through the intermediate state n_1 is then $P_{n_0 \rightarrow n_2} = P_{n_0 \rightarrow n_1} P_{n_1 \rightarrow n_2}$, if the branch point (n_1, n_2) lies to the right of the Stokes line from the (n_0, n_1) branch point. In the other case, it is determined by other branch points.

V. NUMERICAL ILLUSTRATION

The scenario described above was tested numerically on a model Hamiltonian $\hat{H}(X(\tau))$ of the following form:

$$\hat{H} = \cos(X(\tau))\hat{H}_1 + \sin(X(\tau))\hat{H}_2 \quad (5.1)$$

$$X(\tau) = \alpha \tanh(\tau/\alpha) \quad (5.2)$$

where $\tau = \epsilon t$, and \hat{H}_1 and \hat{H}_2 are two independent random square matrices of dimension \mathcal{N} , drawn from the gaussian orthogonal ensemble (GOE). The GOE ensemble consists of real, symmetric matrices with independently gaussian-distributed elements with mean and variance given by [20,21]

$$\langle H_{ij} \rangle = 0, \quad \langle H_{ij}^2 \rangle = (1 + \delta_{ij}) . \quad (5.3)$$

The choice of Hamiltonian is arbitrary, so long as its spectrum is nondegenerate for all real τ , and its eigenvalues and eigenstates become time independent asymptotically as $\tau \rightarrow \pm\infty$. The function $X(\tau)$ was chosen to fulfill the latter requirement. The model (5.1) was used because, for $\mathcal{N} \gg 1$, its spectral properties are representative of those of generic time-reversal invariant multi-level systems [22]. The distance of the branch point singularities from the real axis scales as $\mathcal{N}^{-1/2}$, whereas the singularities of the matrix elements in the complex τ plane have a distribution of positions independent of the matrix dimension \mathcal{N} . It follows that in typical physical applications branch points will lie closer to the real axis than other singularities.

Numerical calculations were performed to determine the ‘exact’ or ‘empirical’ transition probabilities $P_{n \rightarrow m}$ for 100 Hamiltonians of the form (5.1), all with dimension $\mathcal{N} = 6$. In each case all $\mathcal{N}(\mathcal{N} - 1) = 30$ transition probabilities were computed. The scale factor $\alpha = 2$ was assumed in all calculations. The probabilities were obtained by numerical time integration

of the Schrödinger equation, using a standard fourth order Runge-Kutta algorithm with arithmetic accurate to 14 decimal places. Rather than comparing the transition probabilities themselves, we compared (the imaginary part of) the actions times the adiabatic parameter ϵ in units of Planck's constant:

$$\lambda_{nm} \equiv \frac{|\text{Im } S_{nm}|}{\hbar} \epsilon = -\frac{1}{2} \log(P_{n \rightarrow m}) \epsilon . \quad (5.4)$$

The integration was performed between $\tau_i = -25$ and $\tau_f = +25$. We checked that the transition probabilities are insensitive to further increasing the range of τ . These calculations were done for a large set of adiabatic parameters between $\epsilon = 0.001$ and $\epsilon = 0.5$. We observed that in most cases the actions converged to a limit as $\epsilon \rightarrow 0$. In other cases, we estimated the limit by extrapolation with a polynomial. In many cases numerical roundoff error would make the results unreliable for small ϵ . In these cases we assumed the best value for the action corresponded to the smallest value of ϵ for which roundoff errors were not significant. Typically, roundoff errors were significant when the calculated result obeyed $P_{n \rightarrow m} \leq 10^{-23}$. The adiabatic calculations were performed in the following way. First, the approximate locations of the branch points $\tau_{i,j}^*$ were determined by a search for near-degeneracies on a grid in the complex τ plane. The rectangular region bounded by $-6 \leq \text{Re } \tau \leq 6$ and $0 \leq \text{Im } \tau \leq 2$ was usually found to include all the relevant branch points. Next, the locations of these branch point candidates were refined by a version of the Newton-Raphson method adapted to finding square root branch points of the form $E_i - E_j \propto \sqrt{\tau - \tau_{i,j}^*}$. The Stokes and anti-Stokes lines were plotted for several realizations of the random Hamiltonian, and the allowed transition sequences were determined. The Stokes and anti-Stokes lines attached to the branch points were traced by evaluating a sequence of short steps δt along their lengths. If the Stokes line emerging from a branch point between levels i and j was found to pass through the point τ_k , the next point was obtained from $\tau_{k+1} = \tau_k + \delta\tau_k$ where from (2.6) $\delta\tau_k = \epsilon i / [E_i(\tau_k) - E_j(\tau_k)]$, and ϵ is a small real number. Increments of the anti-Stokes lines were determined by an analogous approach. Finally, the ‘adiabatic’ or ‘theoretical’ branch point actions were computed numerically according to

$$\lambda_{i,j} = \frac{1}{\hbar} \left| \text{Im} \int_{(\text{Re } \tau_{i,j}^*, 0)}^{\tau_{i,j}^*} d\tau (E_i(\tau) - E_j(\tau)) \right| . \quad (5.5)$$

The theoretical actions were in excellent agreement with those determined empirically from (5.4). We found that in every case the allowed transition sequence could have been determined by a simple empirical rule, namely, that the real parts of the branch points should be in ascending order. Accordingly, the branch point data were ordered with respect to $\text{Re } \tau_{i,j}^*$. From this ordered table of branch point locations and branch point actions, all possible transition sequences from the initial state n to the final state m , in which the state indices increased (or decreased) monotonically, were considered. According to the rule given in section 2.5, the overall action λ_{nm} was taken to be the least sum of (the imaginary part of) the branch point actions over these possible transition sequences. These calculations of the overall ‘theoretical’ actions were automated.

Examples of the calculations are presented in the tables and figures. Figures 6 and 7 show plots of the energy eigenvalues for real time for two examples of the 100 sample Hamiltonians. The branch point data corresponding to these two cases are listed in tables 1 and 2. Observe

that the avoided crossings in these figures correspond to small values of the branch point actions in the tables. Figures 8 and 9 show the Stokes lines that cross the real axis for all branch points involved in some transition sequence. The ‘theoretical’ transition sequences and actions derived from these data are shown in tables 3 and 4. The ‘empirical’ results obtained using (5.4) are shown there for comparison. Note that the fractional difference between the empirical and theoretical results based on our adiabatic theory is typically around 1% or smaller, although occasionally as high as 2%. The average fractional difference between the empirical and theoretical actions over all 3,000 data points was $\sim 1.6\%$. The data are consistent with the hypothesis that the transition probabilities are given by (1.1) with $C = 1$, and the action S_{nm} given by the topological rule of section 2.5.

VI. CONCLUDING REMARKS

This paper makes three novel contributions to understanding the behavior of the transition probabilities for multi-level systems. First, we have suggested a general rule for determining the combinations of branch points that give allowed transition sequences, based upon an assumption that the transitions occur when a Stokes line, whose dominant solution is occupied, is crossed. Second, we have indicated a general approach to interpreting all of the Stokes lines in a multi-level system, by using a projection technique to selectively remove the most divergent contributions from the renormalized Hamiltonian. And finally, we have verified the rule by means of extensive numerical experiments.

The results of sections 3 and 4 support the rule suggested in section 2, but they do not constitute a proof. Further work must be done to establish how the high order renormalized Hamiltonian can be used to calculate transition probabilities directly in the case of multi-level systems. This might involve studies of how the transition probabilities could be determined by applying time-dependent perturbation theory to the high order renormalized Hamiltonians as t increases along the real axis. This has been successfully applied by Berry [17] for the case of two level systems. An alternative approach would be to investigate analytic continuations of the adiabatic solutions of the renormalized Hamiltonian away from the real axis, as far as the branch points.

There is a theoretical difficulty that must be resolved concerning the interpretation of the Stokes lines. According to the interpretation discussed in section 4, a transition from level n_0 to n_1 occurs on crossing a Stokes line $S(n_0, n_1)$, where the matrix elements $H_{n_0, n_1}^{(k)}(t)$ are greatest for real t . A subsequent transition from state n_1 to n_2 could then occur if the Stokes line $S(n_1, n_2)$ were crossed at a later time. Presumably the allowed transition sequence would then be determined by the order in which the Stokes lines cross the real axis. However, the path in the complex time plane along which the Schrödinger equation is integrated can be deformed away from the real t axis. A problem may arise if the two Stokes lines cross: a transition allowed along one path would then be forbidden along an equally valid path. A rule based on the order in which Stokes lines cross the real axis may therefore predict different transition sequences from the rule in section 2. We have not yet found a totally satisfactory resolution of this problem. We can, however, remark that in our investigations we found no examples where the predictions of the two possible rules were different. It is not clear whether it is impossible to find an example in which the predictions differ, or whether such cases occur with very low probability within our ensemble.

VII. ACKNOWLEDGEMENTS

This work was supported by a research grant, reference GR/L02302 from the EPSRC (UK), and by the program ‘Dynamics of Complex Systems’, at the Max Planck Institute for the Physics of Complex Systems, Dresden. We would like to thank the Nuclear Theory Group at the University of Washington, Seattle and the Max Planck Institute for their hospitality during our visits.

REFERENCES

- [1] M. Born and V. Fock, *Z. fur Physik*, **51**, 165-80, (1928)
- [2] D. Bohm, *Quantum Theory*, Prentice Hall: New York, (1951).
- [3] C. E. Zener, *Proc. Roy. Soc. Lond.*, **137**, 696-702, (1932)
- [4] A. M. Dykhne, A.M., *Sov. Phys. JETP*, **14**, 941-43, (1962)
- [5] J. T. Hwang and P. Pechukas, *J. Chem. Phys.*, **67**, 4640-53, (1977)
- [6] C. E. Carroll and F. T. Hioe, *J. Phys. A: Math. Gen.*, **19**, 1151-61, (1986)
- [7] A. Joye, H. Kunz and C-E. Pfister, *Ann. Phys.*, **208**, 299-332, (1990)
- [8] A. Joye, *SIAM J. Analysis*, **28**, 669-703, (1997)
- [9] S. Brundobler and V. Elser, *J. Phys. A: Math. Gen.*, **26**, 1211-27, (1993)
- [10] E. A. Solov'ev, *Sov. Phys. Usp.*, **32**, 228-50, (1989)
- [11] J. Heading, *An Introduction to Phase Integral Methods*, Methuen: London, (1962).
- [12] J. Heading, *J. Mech. appl. Math.*, **30**, 281-302, (1977)
- [13] G. Stokes, *Trans. Camb. Phil. Soc.*, **10**, 106-28, (1864)
- [14] R. B. Dingle, *Asymptotic Expansions: their Derivation and Interpretation*, Academic Press: New York, (1974).
- [15] M. V. Berry, *Proc. Roy. Soc. Lond.*, **A427**, 265-80, (1990)
- [16] M. V. Berry, *Proc. Roy. Soc. Lond.*, **A429**, 61-72, (1990)
- [17] M. V. Berry and R. Lim, *J. Phys. A: Math. Gen.*, **26**, 4737-47, (1993)
- [18] M. V. Berry, *Proc. Roy. Soc. Lond.*, **A414**, 31-46, (1987)
- [19] J. Von Neumann and E. Wigner, *Phys. Z.*, **30**, 467-470, (1929)
- [20] M. L. Mehta, *Random Matrices*, 2nd ed., Academic Press: New York, (1991).
- [21] F. Haake, *Signatures of Quantum Chaos*, Springer-Verlag: New York, (1991).
- [22] E. J. Austin and M. Wilkinson, *Nonlinearity*, **5**, 1137-50, (1992)

FIGURES

Figure 1. The exponent characterising a non-adiabatic transition in a two-level system is obtained by integrating the energy along a path enclosing a branch point in the complex t plane where the levels become degenerate.

Figure 2. (a) Energy levels as a function of real time for a three level system. The regions where the curves approach each other closely are called ‘avoided crossings’. (b) The avoided crossings correspond to branch points close to the real axis.

Figure 3. (a) The sign of an eigenvector is reversed upon making two circuits about a branch point. (b) Illustrates this change of sign for the Landau-Zener Hamiltonian by considering the eigenvector transported smoothly around a circuit taken to infinity in the upper-half plane.

Figure 4. Stokes lines (S_n), anti-Stokes lines (A_n), and branch cut (BC) associated with a single branch point.

Figure 5. Stokes and anti-Stokes lines associated with a pair of branch points between different pairs of levels. The boundary condition is that only level n_0 is occupied as $t \rightarrow -\infty$. Case (a) allows a transition to level n_2 as $t \rightarrow \infty$. Case (b) does not allow such a transition.

Figure 6. Energy levels for example I of the model Hamiltonian introduced in section 5.

Figure 7. Energy levels for example II of the model Hamiltonian introduced in section 5.

Figure 8. Branch points and Stokes lines intersecting the real axis for example I. The pairs of integers indicate which energy levels become degenerate at each of the branch points.

Figure 9. Branch points and Stokes lines intersecting the real axis for example II.

TABLES

Table 1. Branch point data for example I.

Table 2. Branch point data for example II.

Table 3. Theoretical transition sequences and actions compared with empirical values for example I.

Table 4. Theoretical transition sequences and actions compared with empirical values for example II.

branch point label	state indices i,j	$\text{Re } \tau_{i,j}$	$\hat{\lambda}_{i,j}$
a	5,4	-3.051296	2.637619
b	4,3	-2.739876	.181812
c	2,1	-1.971837	2.918432
d	3,2	-1.791580	.049935
e	6,5	-1.446037	.101999
f	4,3	-1.195295	.119999
g	5,4	-.729159	.031601
h	2,1	-.610604	.024514
i	6,5	-.440841	.267925
j	4,3	-.223932	.256871
k	3,2	.296616	.071114
l	5,4	.668725	.122366
m	5,3	.678210	.480203
n	2,1	.790463	.373673
o	4,3	.884734	.166006
p	3,2	1.242660	.304654
q	6,5	1.609035	2.043553
r	4,3	1.647808	.072687
s	5,4	2.528592	.090388
t	2,1	3.066494	.452725

table 1

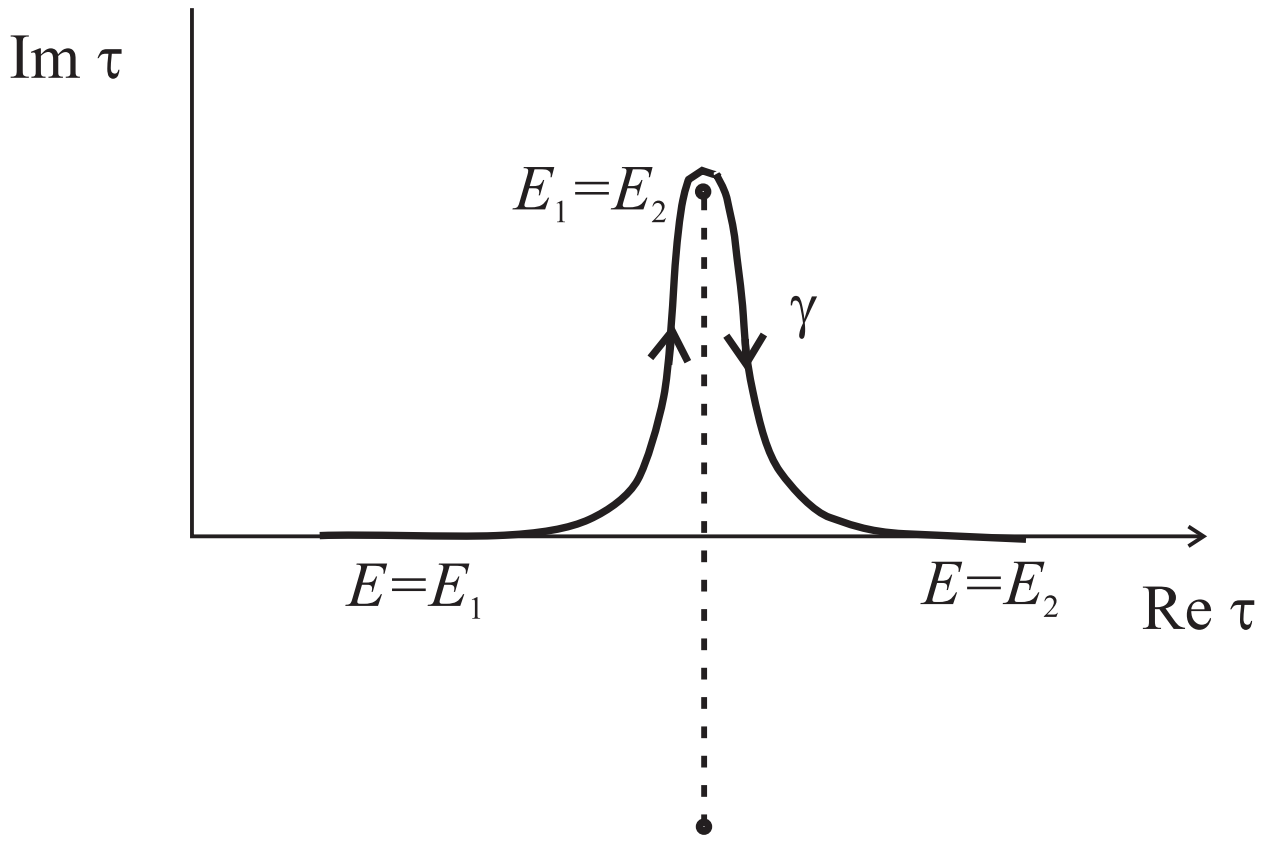


fig.1

branch point label	state indices i,j	$\text{Re } \tau_{i,j}$	$\lambda_{i,j}$
a	4,3	-2.815384	.243081
b	6,5	-2.338206	1.807943
c	2,1	-2.134465	1.915952
d	3,2	-2.065168	.482255
e	6,4	-2.030557	5.220234
f	4,3	-1.809887	.327162
g	2,1	-1.745756	.514480
h	5,3	-1.655970	3.443324
i	3,2	-1.291675	.792717
j	5,4	-1.236497	.019950
k	4,3	-.564900	.028096
l	6,5	.096006	1.027531
m	5,4	.351965	2.323682
n	2,1	.904734	.936584
o	3,2	.965953	.027680
p	3,1	.982541	1.177381
q	4,2	1.037342	1.035606
r	6,5	1.086503	.476258
s	2,1	1.373743	.645514
t	4,3	1.579084	.085708
u	5,4	1.986832	.465658
v	6,3	2.181664	3.069844
w	4,3	2.191573	.428753
x	6,5	2.227829	.770383

table 2

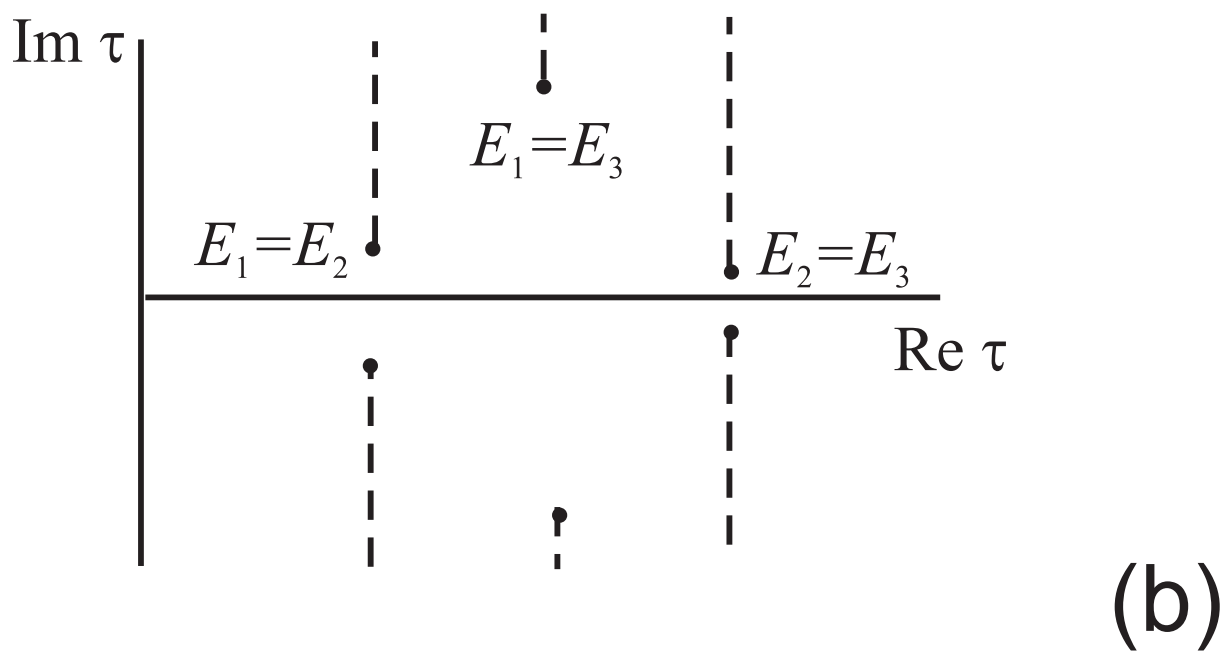
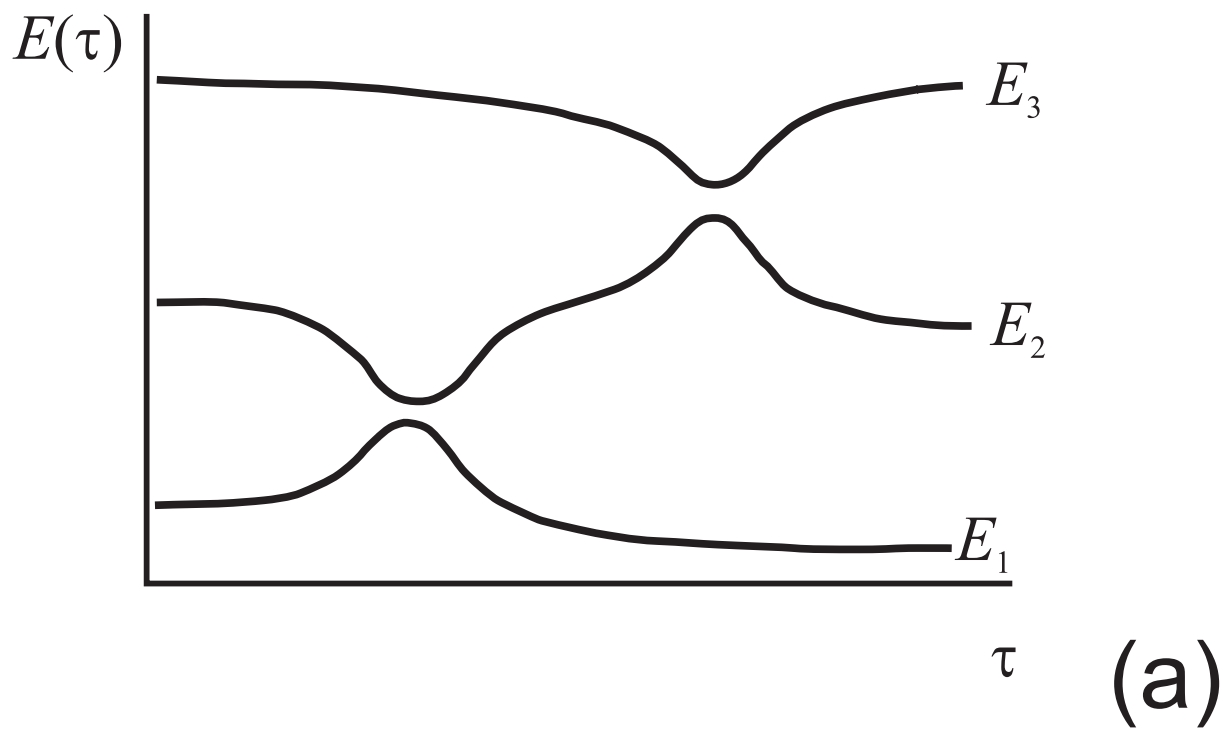
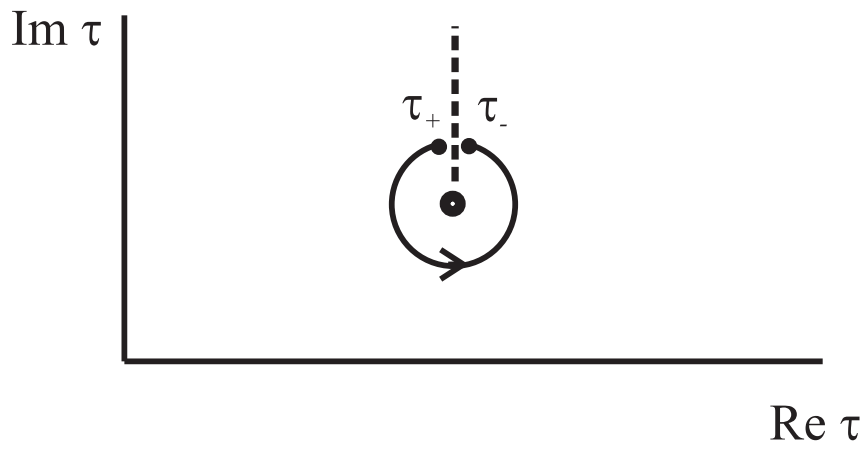


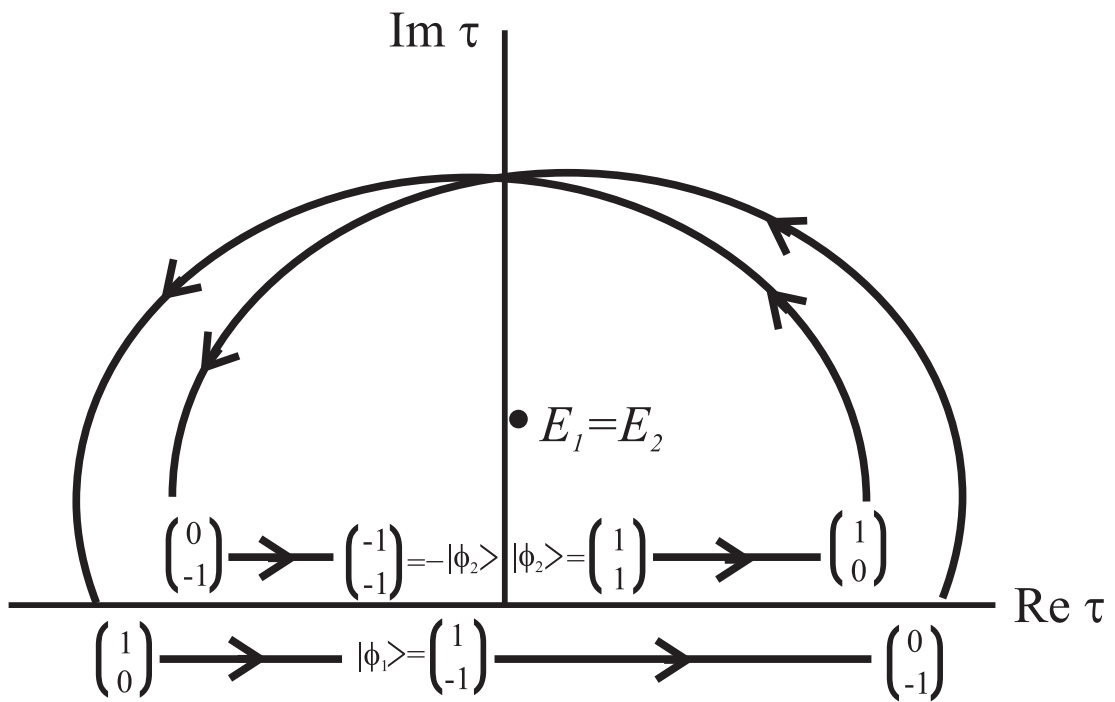
fig.2

Initial state n	Final state m	Transition sequence	λ_{nm} adiabatic	λ_{nm} empirical	Difference	Fractional difference
1	2	h	.024514	.024972	-.00046	-.01833
1	3	h k	.095628	.097049	-.00142	-.01463
1	4	h k r	.168315	.170316	-.00200	-.01174
1	5	h k r s	.258703	.261363	-.00266	-.01018
1	6	h k m q	2.619384	2.630638	-.01125	-.00428
2	1	h	.024514	.024946	-.00043	-.01732
2	3	d	.049935	.050603	-.00067	-.01319
2	4	d r	.122622	.123828	-.00121	-.00974
2	5	d f g	.201535	.204990	-.00345	-.01685
2	6	d f g i	.469460	.473734	-.00427	-.00902
3	1	d h	.074449	.075558	-.00111	-.01467
3	2	d	.049935	.050611	-.00068	-.01336
3	4	r	.072687	.073213	-.00053	-.00719
3	5	f g	.151600	.152904	-.00130	-.00853
3	6	f g i	.419525	.423847	-.00432	-.01020
4	1	b d h	.256262	.257967	-.00171	-.00661
4	2	f k	.191113	.193036	-.00192	-.00996
4	3	r	.072687	.073212	-.00053	-.00717
4	5	g	.031601	.032305	-.00070	-.02181
4	6	g i	.299526	.302137	-.00261	-.00864
5	1	g j k n	.733259	.736357	-.00310	-.00421
5	2	g j k	.359586	.362679	-.00309	-.00853
5	3	g r	.104288	.105613	-.00133	-.01255
5	4	g	.031601	.032305	-.00070	-.02179
5	6	e	.101999	.102708	-.00071	-.00691
6	1	e g j k n	.835258	.846646	-.01139	-.01345
6	2	e g j k	.461585	.465363	-.00378	-.00812
6	3	e g r	.206286	.208215	-.00193	-.00926
6	4	e g	.133599	.134977	-.00138	-.01021
6	5	e	.101999	.102680	-.00068	-.00664

table 3



(a)



(b)

fig.3

Initial state n	Final state m	Transition sequence	λ_{nm} adiabatic	λ_{nm} empirical	Difference	Fractional difference
1	2	g	.514481	.516859	-.00238	-.00460
1	3	g o	.542161	.544292	-.00213	-.00392
1	4	g o t	.627869	.630412	-.00254	-.00403
1	5	g o t u	1.093527	1.098524	-.00500	-.00455
1	6	g o t u x	1.863910	1.870412	-.00650	-.00348
2	1	g	.514481	.516342	-.00186	-.00360
2	3	o	.027680	.028112	-.00043	-.01535
2	4	o t	.113388	.114395	-.00101	-.00880
2	5	o t u	.579047	.581847	-.00280	-.00481
2	6	d f j r	1.305625	1.310825	-.00520	-.00397
3	1	o s	.673194	.677931	-.00474	-.00699
3	2	o	.027680	.028111	-.00043	-.01532
3	4	k	.028096	.028485	-.00039	-.01365
3	5	a j	.263031	.263790	-.00076	-.00288
3	6	a j r	.739289	.742328	-.00304	-.00409
4	1	k o s	.701290	.708465	-.00717	-.01013
4	2	k o	.055776	.056596	-.00082	-.01448
4	3	k	.028096	.028485	-.00039	-.01365
4	5	j	.019950	.020313	-.00036	-.01786
4	6	j r	.496208	.498257	-.00205	-.00411
5	1	j k o s	.721240	.724360	-.00312	-.00431
5	2	j k o	.075726	.076910	-.00118	-.01539
5	3	j k	.048046	.048794	-.00075	-.01534
5	4	j	.019950	.020312	-.00036	-.01784
5	6	r	.476258	.479487	-.00323	-.00673
6	1	b j k o s	2.529184	2.532333	-.00315	-.00124
6	2	b j k o	1.883670	1.888210	-.00454	-.00240
6	3	r u w	1.370669	1.376297	-.00563	-.00409
6	4	r u	.941917	.944955	-.00304	-.00322
6	5	r	.476258	.478059	-.00180	-.00377

table 4

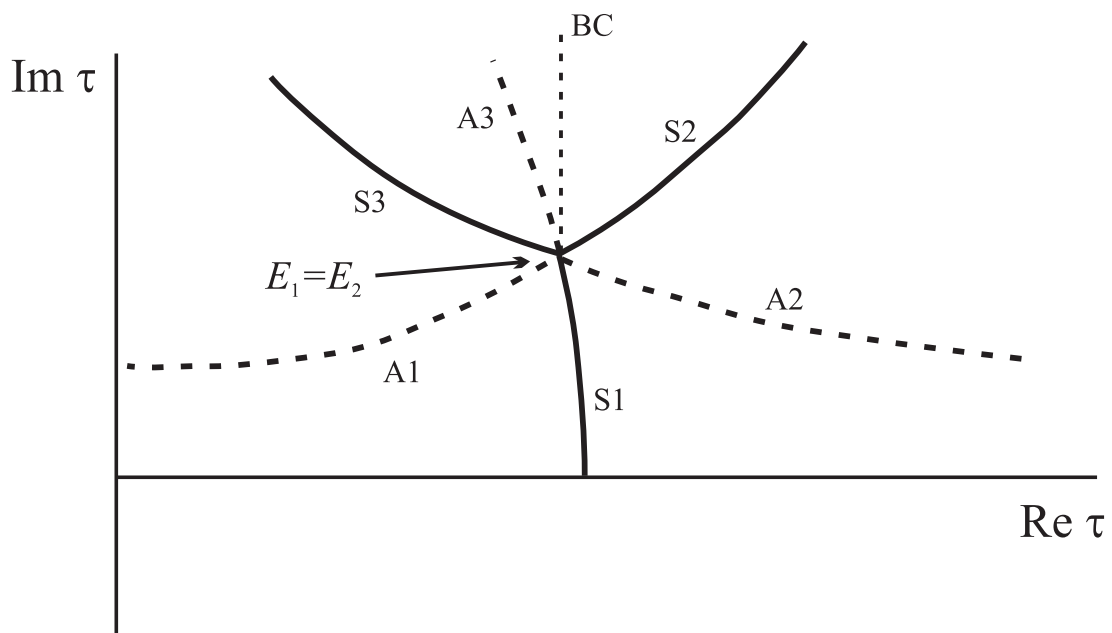
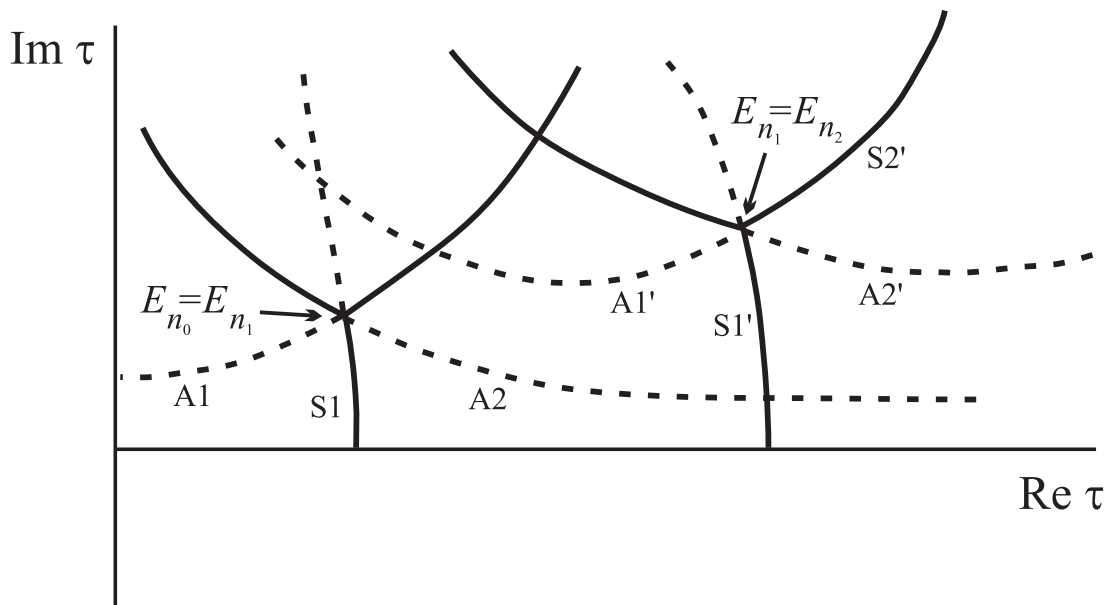
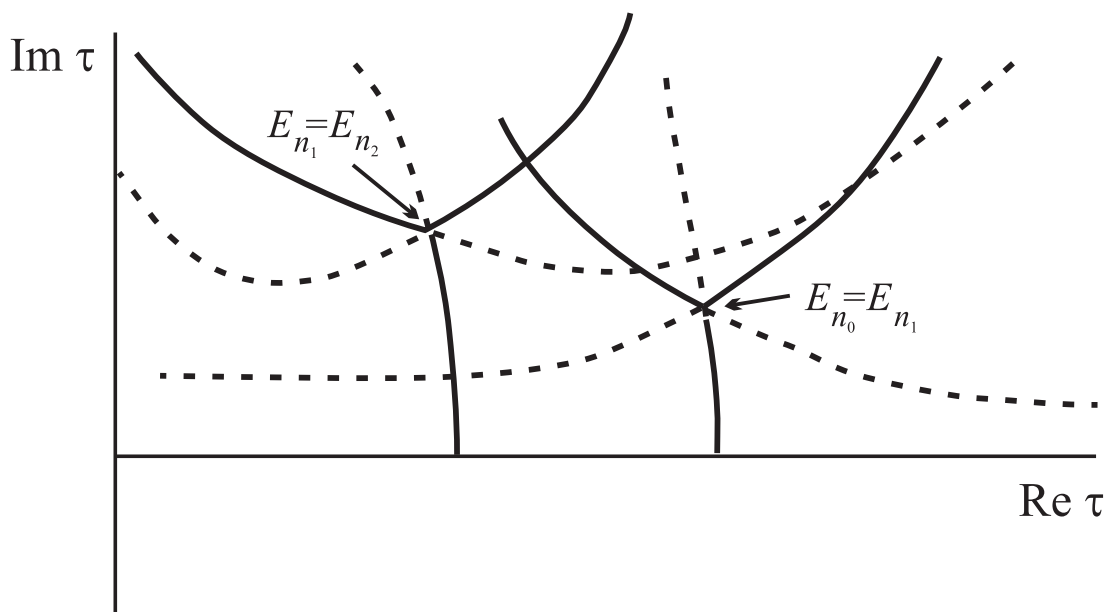


fig.4



(a)



(b)

fig.5

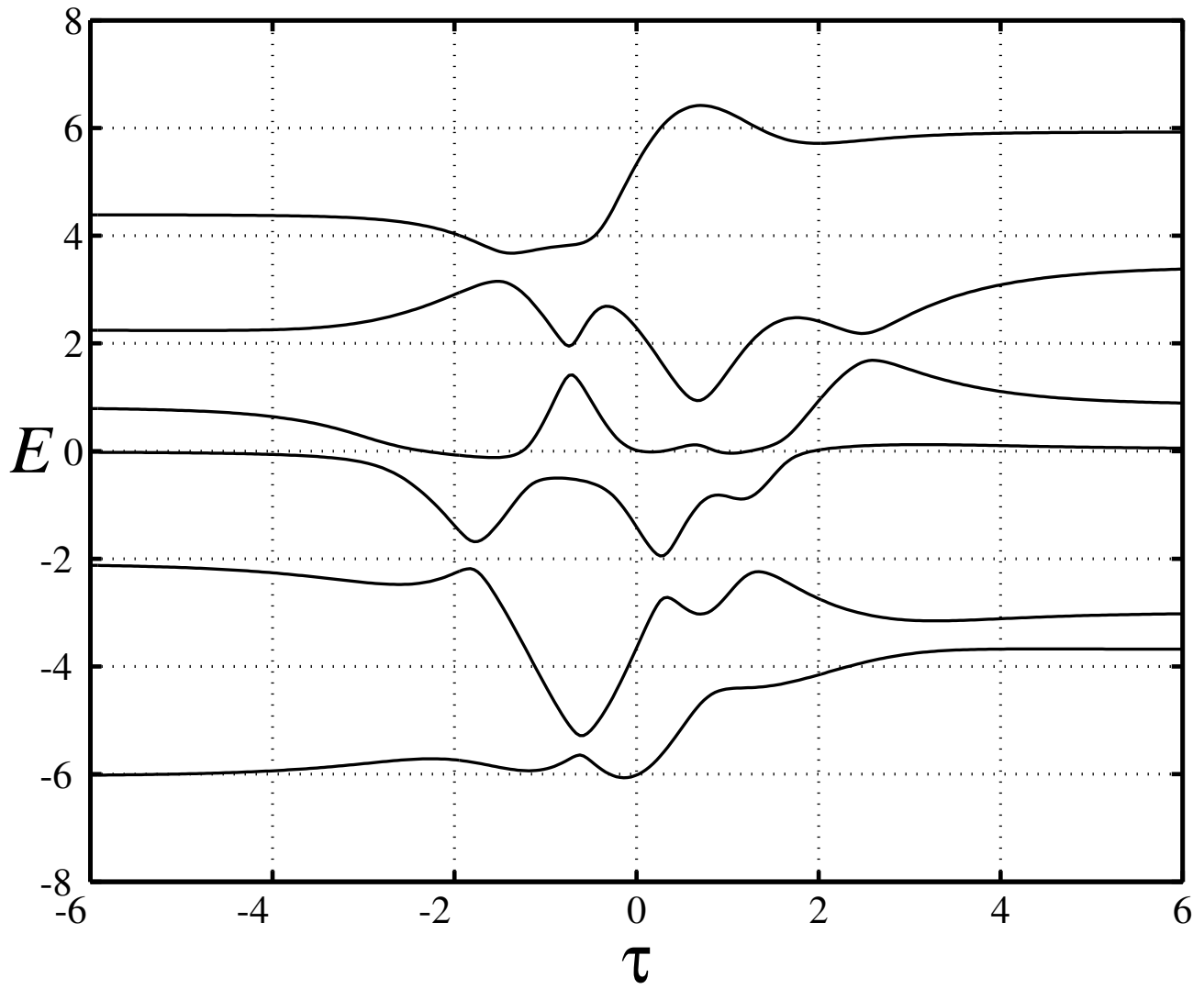


fig. 6

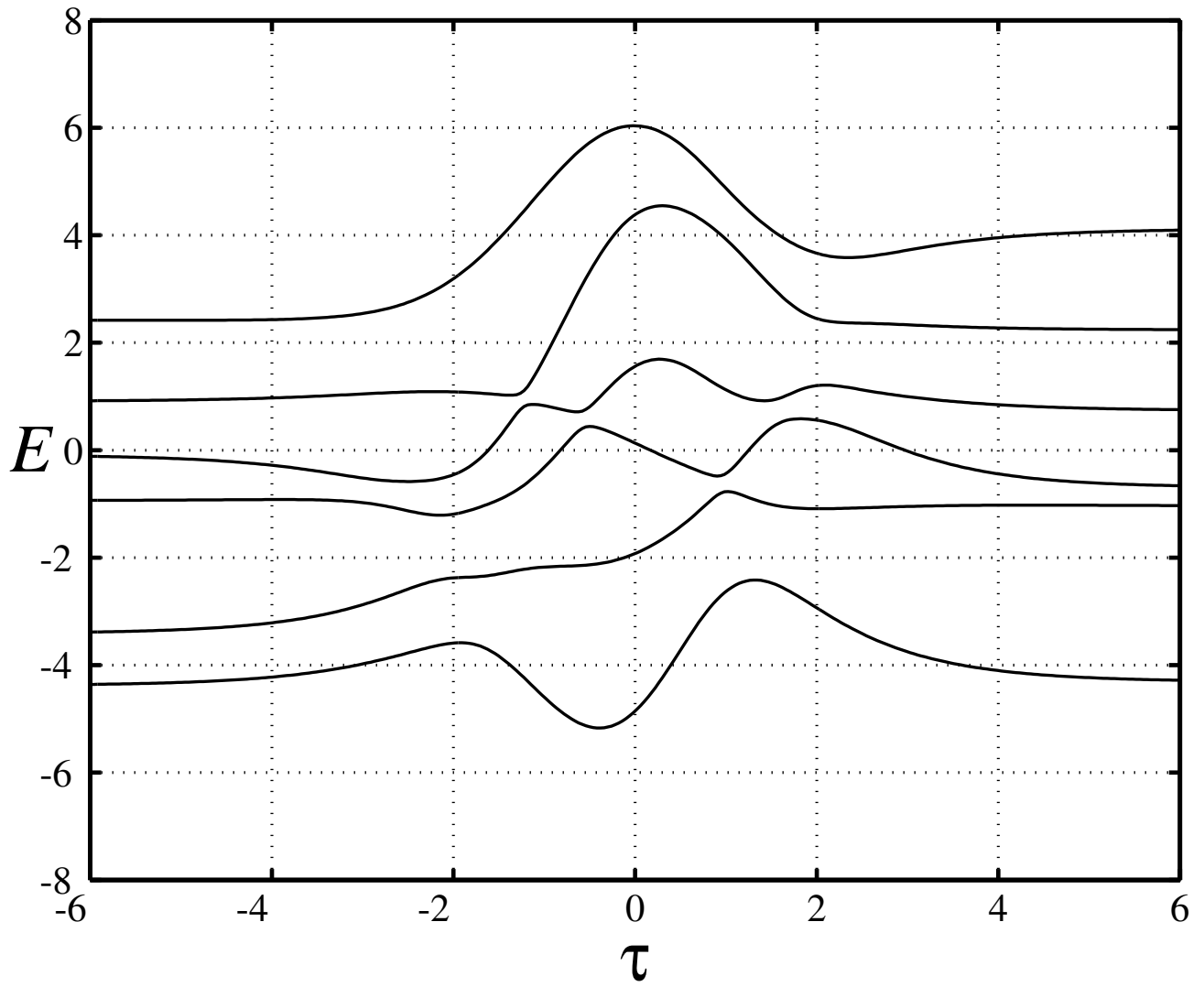


fig. 7

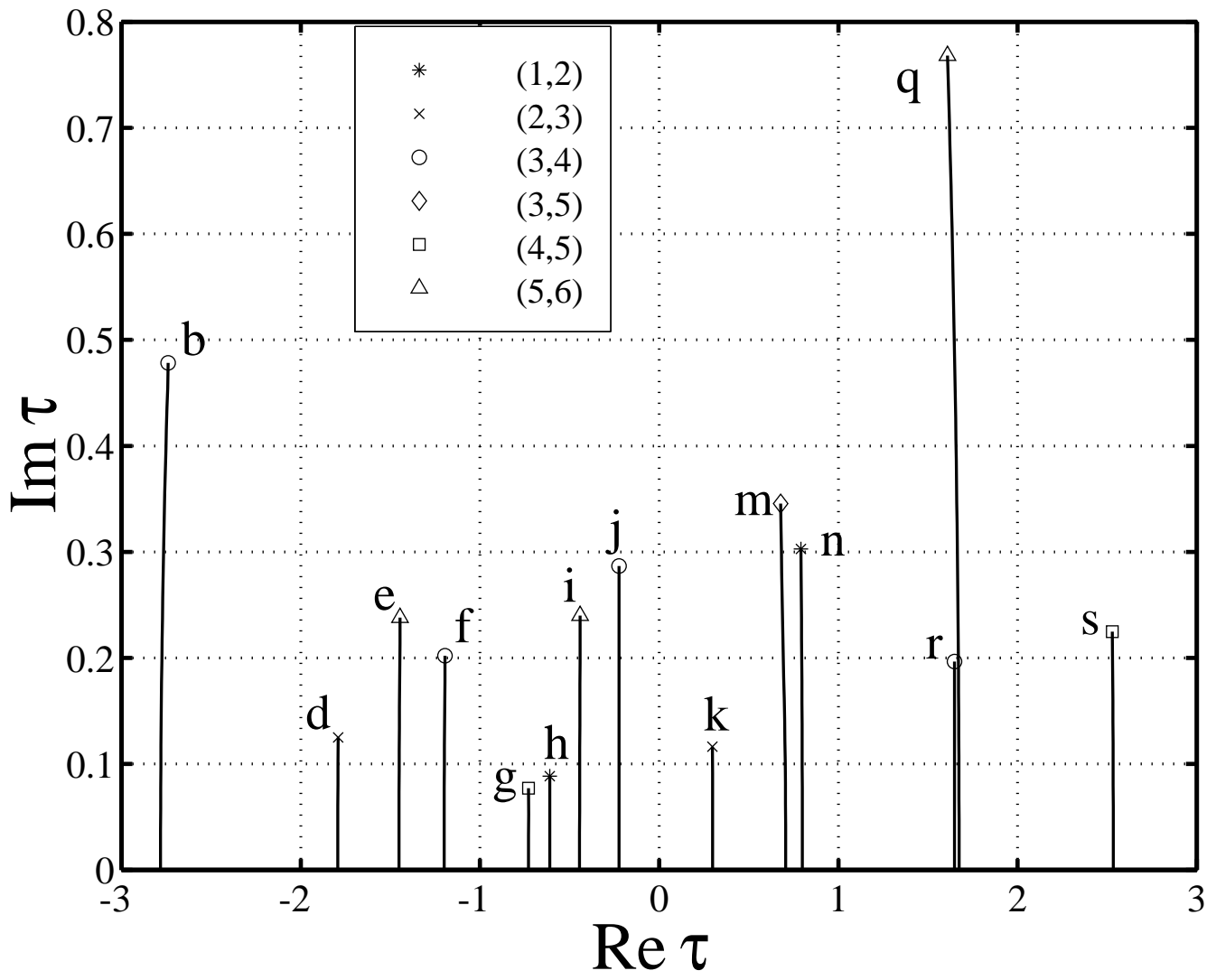


fig. 8

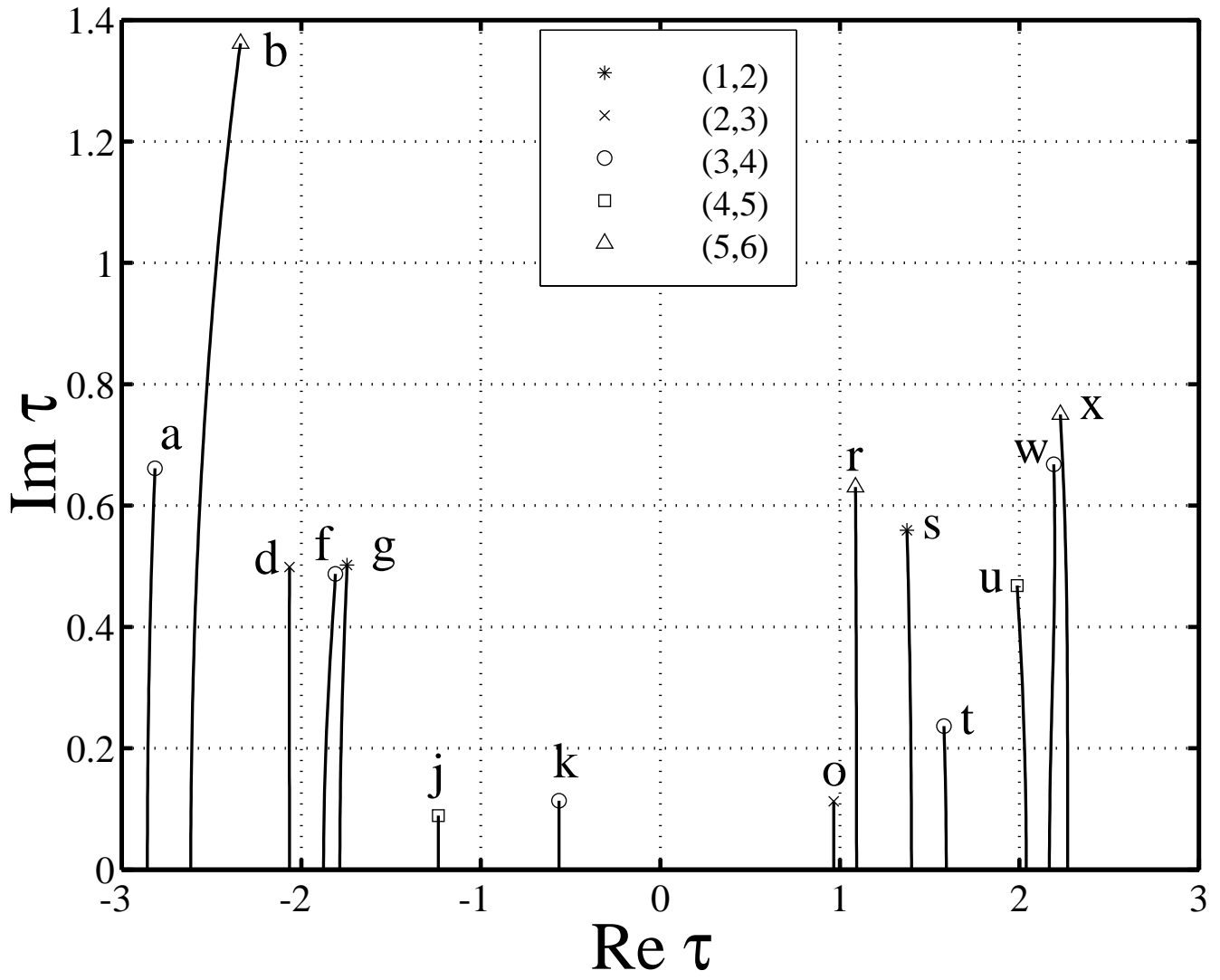


fig. 9